RADIAL AND AXIAL MIXING OF PARTICLES IN A DRY BATCH BALL MILL

Clement Chibwana

A dissertation submitted to the Faculty of Engineering and Built Environment, University of the Witwatersrand, Johannesburg, in fulfilment of the requirements for the degree of Master of Science in Engineering.

November 2005.

STATEMENT OF ORIGINALITY

I declare that this is my own unaided work. It is being submitted for the Degree in Master of Science in Engineering in the University of the Witwatersrand, Johannesburg. It has not been submitted before any degree or examination in any other University.

_____

Clement Chibwana

____day of _____, _____.

Abstract

Mixing is an important operation that is carried out in food, paint, pharmaceutical and mineral processing industries. Ball mills are one of the many mixing vessels used in a mineral processing industry. During grinding, the mill's efficiency depends on particle presentation to the grinding media and the adequate utilisation of the applied forces to effect breakage of particles (ore). Utilisation of applied forces is affected by how well particles and grinding media are mixed. The study of charge mixing is important as it affects the mill's production rate and accelerates media wear, thus relevant to the cost reduction for the milling process.

The kinetics of mixing in a batch ball mill were quantified both radially and axially. Experiments were conducted in a laboratory batch ball mill and two experimental programs were used to study the mixing process. Radial mixing of particles was observed to increase with increasing mill speed. For a mill used in this study, mixing of particles at N_c=90% took almost half the total time taken at N_c=75% to reach completion. A simplified mathematical model is presented, which can be used to predict the radial mixing of particles in a ball mill. Axial mixing of particles was observed to be affected by both the charge system used and segregation of particles from the grinding media. It took a minute for mixing to reach 80% completion for a mill used in the experiments. Mixing of particles was faster in a steel balls/plastic powders charge system than in a glass beads/quartz charge system.

The distribution of particles in a batch mill was observed to vary along the axis of the mill. The centre of the mill was overfilled with particles, $U>1$, while the regions near the mill ends were underfilled, $U<1$. The opposite was true for the grinding media. The data reported was based on measurements of particle distribution along the mill as affected by different charge systems.

The work presented in this thesis is a contribution to the continuing research on mixing of particles in ball mills.

DEDICATION

This work is dedicated to my late Father, sisters Doras and Beatrice. May their souls rest in peace.

Acknowledgements

This work was made possible by contributions and support from different people and organisations.

Prof Michael Moys, my supervisor for the guidance and contributions during the research. You were not only a supervisor but also as a parent.

Mr Murray Bwalya, for the DEM code I used to analyse part of my data. Your work is highly appreciated.

Eskom provided the financial assistance for the project.

Mr Sipho Sekele for your assistance during particle distribution experiments and analysis of data.

Miss Munyewende for your time in editing the manuscript.

My family and Chinkumba for taking all the pain and suffering during my studies. All my friends for the encouragements during trying times.

Prof Moys research group, I learnt a lot from you guys. May you all stay blessed!

Above all, Almighty God for the protection and strength, you lifted me up whenever I was down. I will always praise your name.

TABLE OF CONTENTS

LIST OF FIGURES

LIST OF PUBLICATIONS

1. **Radial mixing of particles in a dry batch ball mill** • **ARTICLE**
   Powder Technology, ***In Press, Corrected Proof****, Available online 22 March 2006,*
   C. Chibwana and M.H. Moys
   Abstract | Full Text + Links | PDF (336 K)

2. **Axial Mixing and Particle Distribution in a Batch Ball;** Chibwana and Moys)

   Powder Technology, Status: Article under review

CHAPTER 1

Introduction

1.0 Introduction

1.1 Mechanisms of grinding

Milling is the last stage of the comminution process in which particles (ore) are reduced to an optimum size range by a combination of impact and abrasion. Impact mechanism occurs when the particle is smashed between a ball and the mill shell and or between the balls. Particle failure is due to compression resulting in fracture. Product particles display a wide range of sizes with disappearance of the parent particle. Abrasion on the other hand is the surface removal of particles due to the rubbing action characterized by the production of fines and yet an identifiable parent particle as the process proceeds.

Milling of particles is usually carried out in conventional ball mills in which steel balls are used as grinding media. The ore is usually fed from one end (feed end) and the product comes out on the other end (discharge end), depending on the design. In the past half century there has been a shift from ball mills to Autogenous mills (AG) and Semi-Autogenous mills (SAG). An AG mill is one in which ore itself is used as a grinding media whereas in a SAG mill apart from using the ore itself as a grinding media, 6-12 % of steel balls by volume are added to aid the milling process.

Despite the shift to AG and SAG, ball mills still remain widely used milling units. The focus of this work is on a dry batch ball mill.

The kinetics of milling depends on:

(a) Particle presentation to sites/regions where it will be subjected to grinding forces.
(b) The application of forces adequate to effect breakage of particles.

In ball mills, the presentation of particles to grinding forces is affected by the degree of particle mixing with the grinding media. There are several factors that can affect

charge mixing in ball mills. These include the speed at which the mill is operated, the size and density of particles being milled relative to the grinding media, mill load i.e. % of ball loading and particle filling, and feed rate including circulation load and water addition flow rate. The above factors affect the mixing rate including the particles residence time distribution and grinding media encounter frequency.

1.2 Thesis objectives

Mixing of particles in the mills is important because it affects the production rates, product size distribution and wear of both lifters and mill liners. The main objectives of this thesis are to study the:

(a) radial mixing of particles in a batch ball mill as affected by mill speed,
(b) axial mixing and transport of particles in ball mills,
(c) effect of different grinding media on mixing kinetics.

1.3 Benefits of understanding mixing in ball mills

Because of the harsh working environment ball mills provide, the milling process has not been well understood (Martin 2001). Understanding of the milling process has been mainly due to observation of inputs and outputs while treating the mill as a black box. Knowledge of particle mixing is therefore important for grinding simulation design and control of ball mills.

1.4 Thesis structure

The thesis starts with a review of literature in chapter 2. The experimental equipments used to measure mixing and the challenges encountered are described in chapter 3. Chapter 4 is dedicated to analysis of radial mixing kinetics. The evolution of mixing index with time as mixing proceeds and the effect of mill's speed on mixing rate are discussed. Mixing of particles in a batch ball mill was simulated using both discrete element methods and diffusion models. Chapter 5 presents the results of axial mixing kinetics.

During axial mixing of particles, it was observed that particles had a tendency of moving away from the front plate. There was thus segregation of particles from the steel balls as mixing proceeded. This behavior was also observed by Clements and Rodgers (1971) and later by Shoji *et al* (1973). In both cases, particle size reduction was assumed negligible during mixing of particles. Chapter 6 presents results of particle distribution along the mill as affected by different grinding media.

The conclusions drawn from this work are presented in chapter 7. Factors affecting mixing and the importance of mixing on ball mill's efficiency are discussed.

CHAPTER 2

Literature Review

2.1 Introduction

Considerable research work has been conducted on mixing of particles in pharmaceutical, mineral processing, ceramics, glass and food industries.

Through investigating various factors that affect mixing, vital information has been reported. These factors include speed (% of critical), fill level (% fraction of the mixer volume occupied by the charge), size and density of particles being processed.

Most research work on mixing has been in pharmaceutical industries where concentration (dosage) control is very important. This is necessary because most drugs are manufactured by combining two or more poisonous elements/compounds. The focus of the work presented in this thesis is mixing in ball mills of mineral processing industries.

Several mixing models have been reported in literature used to predict the extent of mixing. The commonest method however relies on taking measurements of the particles Residence Time Distributions in the mill. The ability of Discrete Element Method (DEM) to predict mixing has also been documented in this thesis.

The measurements of mixing in ball mills may help process engineers understand the mill's production rate, wear rate and circuit control.

2.2 Mixing Process

2.2.1 Definition

For a binary system, a mixture is said to be randomly mixed if the probability of finding a particle constituent is the same at all points in the sample, (Poux *et al* 1991). The above definition is based on statistical approach on mixtures.

2.3 Mechanisms of Mixing

Powder mixing is affected by three mechanisms that may occur simultaneously or separately depending on the mixer design, (Williams 1975). These mechanisms include:

2.3.1 Convection

This is characterised by the motion of particles within the mixture. It is carried out on large scale and results in size reduction of particles.

2.3.2 Diffusion

This is homogenisation by motion of individual particles thereby ensuring mixing on a finer scale.

2.3.3 Shear

Mixing occurs by slipping planes within the whole volume of the mixture.

There are several ways in which mixing of solids differ from mixing of liquids or gases, (Ottino and Khakhar 2000). These are:

(i) Mixing by diffusion mechanism for solids cannot occur without energy input to the mixture.
(ii) In solid mixing, particles to be mixed differ in physical characteristics while in gases and miscible liquids concentration is the main variable.

Due to differences in their physical properties, (size, shape, etc), solid mixtures tend to demix thus making it difficult to achieve a random mixture.

2.4 Types of Mixers

Mixers are classified into different groups according to their design. These include mixers with moving vessels, mixers with fixed vessels and mixers with internal moving parts. Each mixer can be characterised by its predominant mechanism and its mixing action i.e. convection, diffusion or shear, (Poux *et al* 2001).

2.4.1 Shear Mixers

The widely used shear mixer is an industrial ball mill whose main application is in milling. Mixing in a ball is achieved by the tumbling action accompanied by grinding action. Shear mixers are nonetheless inefficient on sticky materials. Another example of a shear mixer is a Pan mixer.

2.4.2 Convection Mixers

Ribbon and High speed impeller mixers are good examples of convection mixers. In a Ribbon mixer, the material are rolled, folded, reversed in direction and literally displaced to achieve the maximum mixing action. The mixer is designed with either one or two ribbons. In a High speed impeller the material spiral upward at the wall of the tank and flow down in the centre of the vessel. Convection mixers are not suitable for materials which are sensitive to heat and there is poor axial mixing of particles.

2.4.3 Diffusion Mixers.

Orbit screw, twin shell, double cone and rotating drum are some of the mixers where diffusion mechanism is dominant. Generally diffusion mixing is accompanied with other mixing mechanisms such as Shear and or Convection. Diffusion mixers are not recommended for materials that tend to agglomerate.

In this study mixing of particles only shear mixers (ball mills) and other diffusion mixers where shear is a dominant mechanism will be discussed.

2.5 Factors Affecting Mixing

Mixing of solids is affected by factors such as:

2.5.1 Size of particles

Size difference can lead to segregation of particles in three ways

2.5.1.1 Trajectory segregation

Consider a particle of diameter, D, and density, ρ_s, which is projected horizontally with velocity, v_o, into a fluid of viscosity, η, then the distance travelled by a particle is given by:

$$d = \frac{v_o \rho_s D^2}{18\eta} \qquad 2.1$$

This distance is called a stopping distance, (Bridgwater 1976).

For particles in a mixer, it is expected that the larger particles will travel a longer stopping distance than smaller ones. This phenomenon will therefore lead to segregation of particles due to size within the mixer charge.

2.5.1.2 Percolation of fines

When a mixture of particles of different size is disturbed such that rearrangement occurs, there is a tendency of small particles to move downwards leading to segregation. The small particles pass through the voids between larger particles when they are at rest. This is known as percolation and can also take place when the bed is vibrated, (Bridgwater 1976).

2.5.1.3 Rise of coarse particles

This is observed when a mixture of coarse and small particles is subjected to a vibration movement. The coarse particles have the tendency of moving up as the fine ones move down. This effect occurs even when the coarse particles are denser than the fine ones. This behaviour has been attributed to the fact that the large particles cause an increase in pressure around the region below it. This compacts the particles and stops large particles from moving down. Thus any upward movement will allow the fines to run under the coarse particles that are later locked in position, (William 1976).

2.5.2 Density

The effect of density difference is similar to the size difference though the effect of size is more adverse than that of density according to Equation 2.1.

2.5.3 Speed of rotation

Different flow regimes have been identified in rotating cylinders depending on the speed of operation, (Nityanand *et al* 1986). Flow regimes are characterised by froude number, *Fr,* given by

$$Fr = \frac{\omega Z^2}{g} \qquad 2.2$$

where g is the acceleration due to gravity, Z is the mixer length and ω is the rotation speed.

For a binary mixture of same density but different size, bigger particles move towards the centre of rotation at low speeds as the small particles move to the mill shell, (Powell and Nurick 1996). As the speed is increased, the behaviour is reversed until around 92% of critical speed when the charge becomes evenly distributed. After 92%

of critical speed, balls will start to centrifuge beginning with the smallest. An opposite trend was observed when particles of same size but different densities were mixed.

Based on the above observations, a model was derived that could be used to obtain optimum combination of size ratio, density ratio and concentration to minimize charge segregation, (Alonso *et al* 1991).

2.5.4 Mixer fill level

Mixing of particles is faster at relatively low fill levels than at higher fill level because of the reduced load turnover time. Load turnover time is the time taken for charge particles to circulate in the mill. Thus at fixed time, particles will circulate more times in a mill of low filling than in higher filled mills, (McCarthy *et al* 1996, Brone *et al* 1998). There is a corresponding increase in load turnover time as the mixer's fill level increases. A fill level beyond 50% leads to progressive central core formation, (region where there is no mixing taking place), and an overall reduction in the rate of mixing.

2.5.5 Surface properties

Surface properties define the behaviour of particles if coherent or adherent. Coherent is defined as the force of attraction between like particles whereas adherent is the force of attraction between unlike particles.

2.6 Types of mixing

The study of mixing can be classified into three groups based on their focus: (a) studies of the time evolution of mixed state (b) studies of axial dispersion (c) studies of radial mixing.

2.6.1 Time evolution studies

These are based on statistical analysis in which mixing indices (see section 2.8 of this thesis) are defined. Different measurement techniques (as described in section 2.7 of this thesis) can be used to determine the degree of mixing.

2.6.2 Axial mixing

This is commonly determined by particle diffusion and it is relatively slow. The axial diffusion coefficient is a parameter that is used to characterise the mixing process in the axial direction and it can be determined both in batch (Shoji *et al* 1973) and continuous (Austin *et al* 1983) operations. The diffusion coefficient can be determined by fitting the experimental data obtained after sufficient rotation time to the diffusion model.

Experimental determination of the diffusion coefficient involves the use of a tracer material at the mill entrance and measuring its concentration as a function of time at the exit. Particle size (Cleary 2003), mill speed (Cleary 2003), and mill filling (Shoji *et al* 1973), are some factors that affect the diffusion coefficient.

2.6.3 Radial mixing

Hogg *et al* (1966) were among the first authors to study radial mixing kinetics using idealised flow models. Particles entering the flowing layer from the bed were assumed to re-enter the bed at the same radial position in the lower half of the layer.

Nityanand *et al* 1986, report that radial mixing usually takes few revolutions compared to axial mixing that takes several hundreds to thousands depending on the mill length. For this reason, it is assumed that radial mixing sets the initial conditions for axial mixing.

2.7 Measurement Techniques

There are several techniques that are used to measure the degree of mixing and most of them have been summarised by Poux *et al* 1991. The main measurement techniques frequently used are:

2.7.1 Thief probe

This is the simplest and most commonly used technique for measuring the degree of mixing. A thief probe is simply a cylindrical rod made of two concentric tubes with pits. These pits can be closed by rotation of the outer tube or by longitudinal slide of a tube. In this method a cylindrical rod is inserted into the mixture and the sample material is allowed to fall under its own weight into one or several pits. The sample is subsequently trapped into the rod by closing the pits before removal from the mixture. The sample can then be examined in order to determine its composition. The method of analysis depends on the nature of particles in the sample. X-ray, fluorescence, analytical methods such as gravimetry, volumetry, electrometry, and particle counting are some of the common methods that can be used.

The disadvantage of using a thief probe is that the insertions may induce perturbations within the mixture thus affecting the results. The continuous removal of samples from the mixture as the process proceeds leads to the depletion of particles in the mixture.

2.7.2 Optic probe

The principle of this technique is based on the requirement that the reflected light from the mixture's surface is dependent on its composition. An optic probe has optic fibres that are inserted into the mixture. Each probe may have two optical fibres i.e. one for sending light into the mixture and the other one for collecting the reflected light from the mixture. The light emitted from the end of the probe is partially

reflected by the mixture and its intensity is measured by a photocell. The measurements of the probe can be accomplished with either visible or ultra-violet light without stopping the mill.

2.7.3 Particle freezing

In some studies powder mixture has been solidified by impregnation with a liquid that polymerises or wax that solidifies. The mixture is then sectioned to the necessary size to form samples that can be analysed. Wightman *et al* (1996) used a mixture of alcohol, water, ocyacdamide, acrylates and butyminomethacrylateco-polymer to solidify the mixture. The process involved careful pumping of the liquid into the mixture, which was followed by controlled drying to avoid bubble formation in the mixture structure. A video camera was used to photograph the mixture and image analysis to quantify the degree of mixedness.

Depending on the nature of particles, the use of impregnates or liquids might dissolve or disturb the mixture thus affecting the results.

2.7.4 Coloured particles

This technique is very much similar to the optical probe and was first proposed by Bannister and Harnby (1983). Coloured particles are introduced into a vessel with clear walls, which already contain particles of different colour. Rapid photographs taken at close range, which can be analysed by an automatic Colour –Eye spectrometer, may be used to quantify kinetics of mixing. A particle velocity distribution map that describes the movement of the tracked materials can then be generated.

The main disadvantage of the above method is that it does not give details of the mixing process along the axis of the mill and therefore the data collected is restricted to the measurements done from the end walls.

2.7.5 Radioactive

In this method a radioactive substance is used to track the mixing of solids and liquids. Some of the mixture components are made radioactive by chemical activation. Mixing can be quantified by either discrete sample counting, use of thief probe, or continuous counting in which scintillation detectors may be used by inserting them in a mixture (Austin *et al* 1983).

Radioactive method is normally discouraged because of:

(1) The cost associated with the process
(2) Strict safety rules associated with the use of radioactive substances.

2.8 Measuring Mixing

2.8.1 Concept of mixing index

A mixing index is a measure of a degree of mixedness or randomness. A useful index should have the following properties:

(1) independent of a mixing process
(2) easy to determine
(3) closely related to specify the characteristics of the final product.

Several mixing indices based on different criteria have been summarised by Fan *et al* (1990). The criteria used to determine indices were based on either statistical analysis, calculating the standard deviation of the sample, or experimental work.

2.9 Residence Time Distribution (RTD) of Particles in mills

2.9.1 Definition:

Consider a steady-state feed into a reactor and let some fraction of the feed admitted over a very short time, Δt, be marked with a tracer of some kind. If the tracer presence is tested at the exit stream and if $\Phi(t)$ defines the accumulative mass fraction of tracer mass at the exit, then at time t after the traced feed entered, a fraction $1-\Phi(t)$ will still be inside the mill, (Austin *et al* 1984).

$$\left.\begin{aligned}\Phi(t) &= 0, 0 \le t \le \tau \\ \Phi(t) &= 1, t \ge \tau\end{aligned}\right\} \text{ Plug flow} \qquad 2.3$$

$$\Phi(t) = 1 - e^{-\frac{t}{\tau}}, 0 \le \tau \quad \text{Fully mixed.} \qquad 2.4$$

In which τ is the mean residence time defined as:

$\tau = \frac{W}{F}$ where F is the powder feed rate and W is the mill hold-up.

Equation 2.3 therefore defines the sudden emergence of all traced material after a mean residence time in which there is no forward or back mixing as the material flows in the mill. In a fully mixed system however, Equation 2.4, the tracer mixes with the bulk material immediately it is introduced into the mill.

The above definition assumes that the powder in the mill disperses mixes and flows independent of the particle size, shape and density.

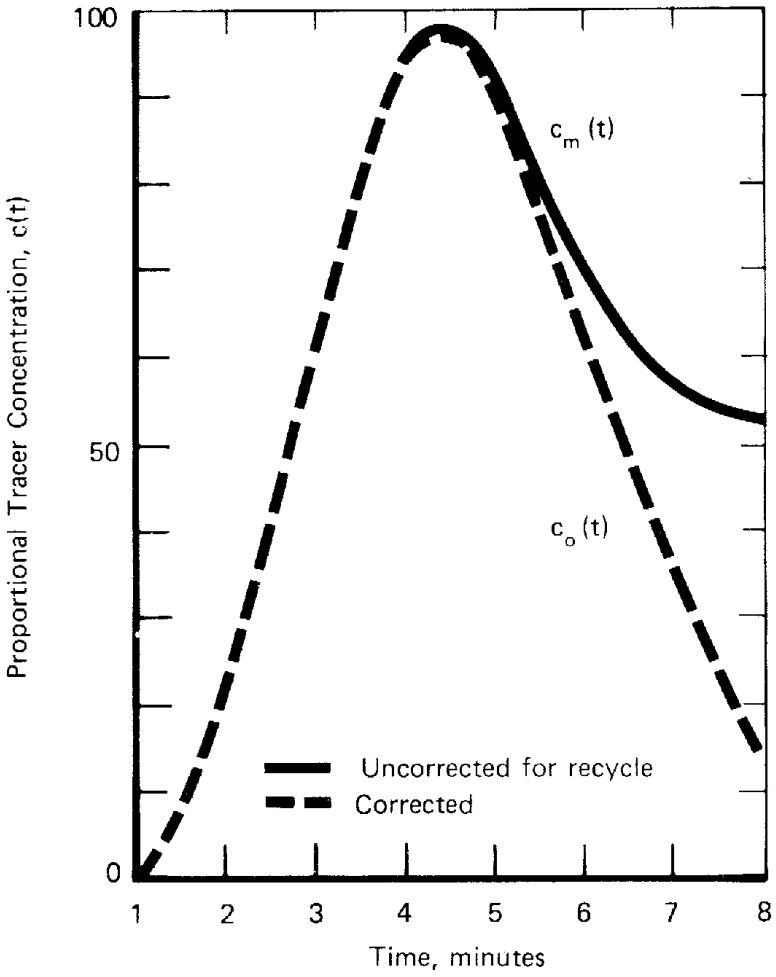

Figure 2.1 showing tracer at the mill exit at time t after a pulse of tracer addition to mill feed for a closed circuit from Austin *et al* (1984)

2.9.2 Determination of RTD

Practical determination of RTD in a mill can be achieved by measuring the values of tracer concentration, *c(t),* in the mill exit stream at time *t*. A sample of tracer material is collected over a short sampling period and analysed for comparative tracer content, Figure 1. For a mill operating at steady state with material flow rate, *F*, the amount of tracer that has left the mill at time *t* after admission is proportional to

$$\int_0^t c(t)Fdt \qquad 2.5$$

The total amount of tracer that will have left a mill after along time of mixing will be equivalent to:

$$\int_0^\infty c(t)Fdt \qquad 2.6$$

These expressions are valid for an open-circuit operated mill.

If on the other hand a closed circuit is used, then a correction factor for the tracer content from the classifier recycle stream must be incorporated in the equation. The total amount of tracer leaving the mill will therefore be given by:

$$c(t) - c_o(t) = \frac{C}{1+C}\int_{\theta=0}^{\theta=t} \Phi(t-\theta)c_R(\theta)d\theta \qquad 2.7$$

where $c(t) =$ tracer concentration measured after time *t* of admission

$c_o(t) =$ initial tracer concentration.

$C =$ circulation ratio

$c_R(\theta)$ = tracer proportion in the recycle stream

$\Phi(t-\theta) =$ tracer fraction per unit time from $\theta - \theta + t$

The technique employed in the determination of RTD depends on the nature of ore being treated (conducting or non-conducting) and the milling process itself (dry or wet and closed or open).

In wet milling it is normally assumed that the pulp density of the slurry is constant so that the residence time of the powder is the same as that of water. Estimation of the RTD values may be achieved by the addition of a soluble tracer to water provided the tracer cannot be adsorbed on the solids of the mill contents. For minerals with low conductivity, NaCl or KCl can be used as a tracer. In this method the tracer concentration can be measured by using conductivity cells (Martin 2001).

In dry milling, flourescein can be used to determine the RTD, (Mardulier and Wightman 1971). The flourescein solution is absorbed on the micro-porous structure of the solid particles thereby leaving a dye coating on the internal pores. When the dyed particles are introduced into the mill, their concentration can be determined at the mill exit by sampling at specific time intervals. A photoflourometer with an accuracy of one part per 10^8 parts of sample can be used to determine the flourescein concentration. The advantage of determining the particle RTD in dry mills is that it eliminates the assumptions concerning solid's pulp density and tracer adsorption on solids.

Radiotracing by neutron irradiation of a sample of the solid to make it radio active, with count rate measurements by Geiger-Muller tube or NaI photomultiplier detectors, has been used successfully, (Austin *et al* 1983). Samples are collected for counting by detectors placed at various point along the mill length to pick up emitted radiation from the issuing stream. Detectors may also be placed in a discharge sump and cyclone underflow discharge for a closed circuit.

2.10 Mixing Models

There are several methods that have been used to model mixing of particles both in the radial and axial directions. These are:

(1) Monte Carlo simulations
(2) Discrete element method

(3) Finite stage transport
(4) Dispersion model

2.10.1 Monte Carlo Simulations

Several authors have used this simulation method to model mixing of particles. It is simply a mathematical experiment by which the expected outcome of the stochastic process is estimated by the random sampling from the probability distribution that governs the events making up the process- (Sherritt *et al* 2003).

Cahn and Fuerstenau (1967) considered a bed of particles that circulates in a plane perpendicular to the drum axis. The bed was treated to have a rotational speed that was greater than the drum speed. The drum was divided into sections of equal width perpendicular to the axis. A Monte Carlo simulation was used to model the axial movement of particles between the sections. The three probability distributions considered were:

(a) the number of particles that leave the section per bed revolution
(b) the direction the particles move
(c) the axial distance the particles move

There was good agreement between the model predictions and axial mixing observed in the non-flow experiments.

Rodgers and Gardner (1979) assumed that a particle moved on a fixed radius until it reaches the bed surface. On the bed surface, the particle is free to tumble or roll until it re-enters the bed at a new radius. There is inter-particle collision while the particle is on the bed surface. Due to the collision, the angle at which the particle descends deviates from the angle of maximum descent. The particle's radial position determines the time and distance it will take on the bed surface before it re-enters the bed. The angle of descent determines the axial movement of the particle.

The two probability distributions used in the Monte Carlo simulations are:

(a) the radius at which the particle re-enters the bed is a uniform distribution weighted for the number of particles at each radius and
(b) the angle of descent has a normal distribution about the angle of maximum descent. The standard deviation for the angle is determined at various fill levels from non-flowing experiments-(Shoji *et al* 1973).

Experimental data from Shoji *et al* (1973) was compared with the simulation predictions from Rogers and Gardner (1979). A good agreement was observed between the experimental and model predictions.

A Monte Carlo simulation can give good predictions of the axial mixing if the significant events are included. One disadvantage of this simulation method is the large amount of computing time required and the properties of the distributions must be specified. There have been no attempts made to relate the probability distribution of the events with parameters such as mill speed, fill level, mill diameter and particle properties.

2.10.2 Discrete Element Method – DEM

Mishra and Ramajani (1993) pioneered the use of DEM in mineral processing. In this simulation method, collisional interaction of particles with each other and their environment are modelled. It uses the soft particle method. Particles are allowed to overlap and the amount of overlap, Δx, normal velocity, v_n, and tangential velocity, v_t, relative velocity determine the collisional forces. A conventional linear spring-dashpot model is used in DEM simulations.

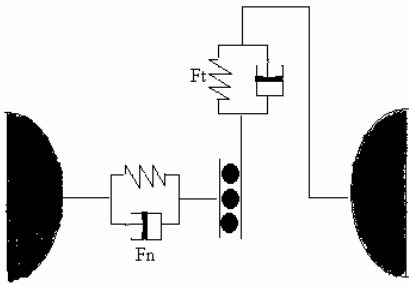

Figure 2.2 The contact model involves a spring and dashpot in the normal direction and an incrementing spring and dashpot limited by the sliding friction in the tangential direction.

The normal force,

$$F_n = -k_n \Delta x + C_n v_n \qquad 2.8$$

consists of the spring to provide the repulsive force and a dashpot to dissipate a proportion of the relative kinetic energy. The maximum overlap between particles is determined by the stiffness k of the spring in the normal direction. The normal damping coefficient is chosen to give a required coefficient of restitution ε (ratio of the post-collisional to pre-collisional normal component of the relative velocity):

$$C_n = 2\gamma\sqrt{m_{ij} k_n} \qquad 2.9$$

where $\gamma = -\dfrac{\ln(\varepsilon)}{\sqrt{\pi^2 + \ln^2(\varepsilon)}}$ and $m_{ij} = \dfrac{m_i m_j}{m_i + m_j}$ 2.10

is the reduced mass of particles i and j with masses m_i and m_j, Cleary 1998.

The tangential force is given by:

$$F_t = \min\left\{\mu F_n, k_t \int v_t dt + C_t v_t\right\} \qquad 2.11$$

where the integral velocity v_t over the collision behaves as an incremental spring that stores energy from the relative motion and represents elastic tangential deformation of the contacting surfaces. The dashpot dissipates energy from the tangential motion and models the tangential plastic deformation of the contact. The total tangential force (given by the sum of plastic and elastic components) is limited by the coulomb frictional limit at which point the surface contact shears and the particle begin to slide over each other. The contact model requires that both the coefficient of elasticity and friction of particles to be supplied.

The DEM algorithm has three essential parts:

(a) a search grid is used to periodically build a particle near-neighbour interaction list with boundary objects appearing as virtual particles. In this way the force computation operation is minimised.
(b) The collisional forces on each of the particles and boundary objects are evaluated efficiently using near neighbour list and the spring dashpot interaction model and then transformed into a simulation frame of reference.
(c) All the forces on each of the objects and particles are summed and the resulting equation integrated

DEM has been used to simulate power (Mishra and Ramajani -1989), liner wear (Kalala and Moys 2002) and granular flows (Cleary 1998). DEM predictions were compared with experimental data to study the effect of fill level and particle size for slowly rotated cylinders (Cleary 2000). It was also used to study the factors affecting diffusion coefficient in the axial transport of particles (Cleary 2003).

2.10.3 Finite Stage Transport (reactor in series)

The reactor-in-series model can also be used to establish the empirical description of Residence Distribution Time (RTD). In this method the experimental RTD is matched against a theoretical expression derived for a number of fully mixed reactors and the number of proportional sizes giving the best match chosen.

If the axial mixing is small (like in rotary kilns), the number of mixers, *m*, can be approximated from the mean residence time <*t*> and the standard deviation of the residence time, $\sigma^2{}_t$, as given below:

$$m = \frac{< t >^2}{\sigma^2{}_t} \qquad 2.12$$

For *m* fully mixed mixers with the same residence time, the differential RTD, $\phi_m(t)$, is given as:

$$\phi_m(t) = \frac{t^{m-1}}{\bar{\tau}(m-1)!} e^{-\frac{t}{\bar{\tau}}} \qquad 2.13$$

$$\text{where } \bar{\tau} = \frac{t_p}{m-1}, \qquad \& \qquad \tau = t_p \frac{m}{m-1} \qquad 2.14$$

where t_p is the time at which the tracer concentration reaches its peak.

This simulation model can be used to approximate 100 or more perfectly mixers in series thus approximating a typical industrial mixer (ball mill, kiln) with a length-to-diameter ratio of 10. The disadvantage of this method is that it cannot be used to predict axial mixing in batch experiments, (Levenspiel 1972).

2.10.4 Dispersion Model

2.10.4.1 Continuous Operation.

This is the most widely used model for describing axial mixing of particles.

Definition:

Consider a mill operated at steady state with particle filling along the mill being almost constant, then the movement of a traced material can be described in two ways:

(i) the flow of traced material at constant bulk flow velocity and
(ii) the superimpose dispersion or diffusion effect due to the mixing action of the mill

Thus if a traced material is considered to diffuse at the rate dependent on the partial concentration in the bulk of the material, then Fick's law of diffusion may apply, i.e.:

$$\frac{\partial c}{\partial t} = D\frac{\partial^2 c}{\partial z^2} - v\frac{\partial c}{\partial z} \qquad 2.15$$

where c is tracer concentration (gram tracer per gram solid), D is diffusion coefficient (m^2/s), v is the linear velocity (m/s) of particle flow in the z direction (m) of the mill after time t.

The axial dispersion model has the following advantages

(i) There is no restriction to the number particles to be used in the charge.
(ii) A single parameter, dispersion coefficient, can be used to quantify the rate of mixing in the axial direction.
(iii) The dispersion can be determined from either continuous or batch experiments.

The dispersion coefficient is usually determined by fitting the diffusion equation above to the experimental data.

The main disadvantage of the dispersion model is that it assumes particle transport to be independent of size. This is valid in cases where there is negligible particle breakage. In most cases however, particle transport is accompanied by particle breakage and as such it should incorporated in the diffusion equation.

Consider a transverse axial slice of length *dz,* then the general mass balance of particle of size *i* can be given as:

The rate of increase of particle mass of size *i* material in the slice = (dispersion and diffusion fluxes of size *i* entering the slice) + (sum rate of production of *i* from the breakage of size larger than *i* in the slice) – (rate of disappearance of size *i* in the slice) - (dispersion and diffusion fluxes of size i leaving the slice), Rogovin and Hogg (1988).

Mathematically:

$$\frac{\partial[W(z)c_i(z)]}{\partial t} = D_i \frac{\partial^2[W(z)c_i(z)]}{\partial^2 z} - v_i \frac{\partial[W(z)c_i(z)]}{\partial z} - S_i W(z)c_i(z) + \sum_{\substack{j=1 \\ i>1}}^{i-1} b_{ij} W(z) S_j c_j(t), \quad \text{for } n \geq i \geq j \geq 1 \qquad 2.16$$

where

$W(z)$= mill hold-up per mill unit length at point z

$c_i(z)$= concentration of particle size class i

D_i=diffusion coefficient of size i

v_i =axial velocity of size i

S_i= specific rate of breakage of size *i*

b_{ij} = breakage function of size j into *i*

z= mill's axial location

n = smallest particle size range.

At constant mill hold-up the above equation can be written as:

$$\frac{\partial c_i(z)}{\partial t} = D_i \frac{\partial^2 c_i(z)}{\partial^2 z} - v_i \frac{\partial c_i(z)}{\partial z} - S_i c_i(z) + \sum_{\substack{j=1 \\ i>1}}^{i-1} b_{ij} S_j c_j(t), \qquad 2.17$$

2.10.4.2 Batch Operation

For batch experiments, there is no net flow of material in the axial direction and as such equation 2.15 reduces to:

$$\frac{\partial c}{\partial t} = D \frac{\partial^2 c}{\partial z^2} \qquad 2.18$$

Sherritt *et al* 2003, summarises the solutions that can be used to determine the dispersion coefficient for different initial conditions.

2.12 Axial particle distribution in mills

Transport of materials through ball mills can be affected by classification of particles within the mill. This classification is due to particle size and maybe classified as either exit or velocity classification

2.12.1 Exit Classification

This occurs in ball mills and semi-autogenous mills with grate discharge whose duty is to prevent coarse particles from exiting until they break to a certain size. The size distribution near discharge was found to be coarser and narrower than the inner location while the discharge is finer than the mill contents, (Rogovin and Hogg 1988, Chom and Austin 2004).

2.12.2 Velocity Classification

This is affected by the size of the particles within the mill. Velocity classification can either be size independent or size dependent (Rogovin, Z and Hogg R 1988). The first case occurs when there is negligible size reduction and as such particles are assumed to have the same flow velocity and dispersion coefficient (Rogovin, Z and Hogg R 1988).

In size dependent flow, coarse particles are expected to move slower than fine particles in wet overflow ball mills. This is because the fine particles can easily be washed away by the slurry as it flows through the mill. The discharge size distribution is therefore finer than the mill contents.

In dry mills however, coarser particles may move axially faster than the fines. This is due to the fact that coarser particles have higher momentum and therefore they cover a longer distance before they stop than fine particles as they cascade down the free surface. Also the chances of coarser particles getting trapped into the voids of grinding media are slimmer than that of fine particles. Due to this, the size distribution of the product is expected to be coarser than that of any axial location inside the mill. Rogovin and Hogg (1988) showed that the mill hold up increases from mill feed end to the discharge end experimentally.

The consequences of internal classification for the size reduction process are:

(i) Retention of particles in mills varies with size

(ii) Mill size distribution differs discontinuously from that of the mill content.

2.14 Conclusions

Literature on mixing of particles has been presented. It is evident that most work on mixing has been conducted with particles of same size but different colours operated at very low speeds. Measurements of particle mixing and their transport in ball mills still offers a challenge because of the harsh working environment mills present. The work presented in this thesis is a contribution to the understanding of mixing in ball mills operated at typical industrial speeds.

CHAPTER 3

Experimental Apparatus and Programs

3.0 Introduction

This chapter discusses the experimental programs used in this thesis. Two experimental methods were used to measure particle mixing in a batch mill. In the first method, measurements of particle mixing were achieved by capturing the process on video. This was made possible by using a transparent front plate on the mill. The second method involved the dividing of the mill load into 4 sections whose contents were gravimetrically determined as a function of time.

Method of data analysis, mill controls and its description are also discussed in this chapter.

3.1 Experimental Procedure 1

3.1.1 Description of the Laboratory batch mill.

The experiments were carried out in laboratory mill that was mounted on a rig for precise control and experimentation. The mill, shown in Figure 3.1, has an internal diameter of 0.54m and an internal length of 0.4m. The interior of the mill was lined with 12 trapezoidal lifters with 45^{o} base angles, Figure 3.2. The end wall was made of steel plate while the front plate was made of transparent 12mm thick Perspex so that the mixing process could be filmed. The front plate was firmly fastened to the mill with steel bolts for easy removal. In order to ensure that the mill was dust / particle proof, a rubber liner was placed between the front plate and the mill shell.

The rig was designed to drive any mill that can draw power less than 3KW. The mill was mounted on a conical flange attached to the axle drive of the rig. The mill was flanged to an axle that both supported the mill and rotated it. The axle turned in large bearings attached to the supporting frame. The motor and gear box were suspended in the cage below the mill by bearings. Power from the motor was transmitted to the axle via a drive chain. The mill's

speed could be varied from 0-200% of the critical speed with minimum variations from the set speed.

The room was sufficiently illuminated during the experiments. This was achieved by the use of two light sources supplied by 500W projectile halogen lamps. Lighting conditions were maintained throughout the experiments by fixing the lamp positions. This was important because the method adopted in this thesis for data analysis depends on the amount of light reflected by the image. Thus any variation in light during experiments can adversely affect the results of the analyses.

A Panasonic Digital Camera, NV-GS3EN, was positioned about 2m away from the mill's front plate. This Camera operating at 25frames/sec was used to film the events from the end window as mixing proceeded.

The charge to the mill comprised steel balls and plastic PVC powders. The steel balls were in the size range of 6 – 10 mm with density of 7800kg/m^3. The plastic powders had a mean diameter of 300μm, density of 939kg/m^3 and slightly cohesive (data supplied by manufacturer).

The mill length was easily adjusted to the desired length during the experiments. This was achieved by the use of a partition plate and steel rods which were fastened at the back of the mill. This made it possible to carry out both axial and radial experiments in the same mill. The length of the mill was adjusted to 100mm for all radial mixing experiments whereas a full length mill, 400mm, was used for axial mixing experiments.

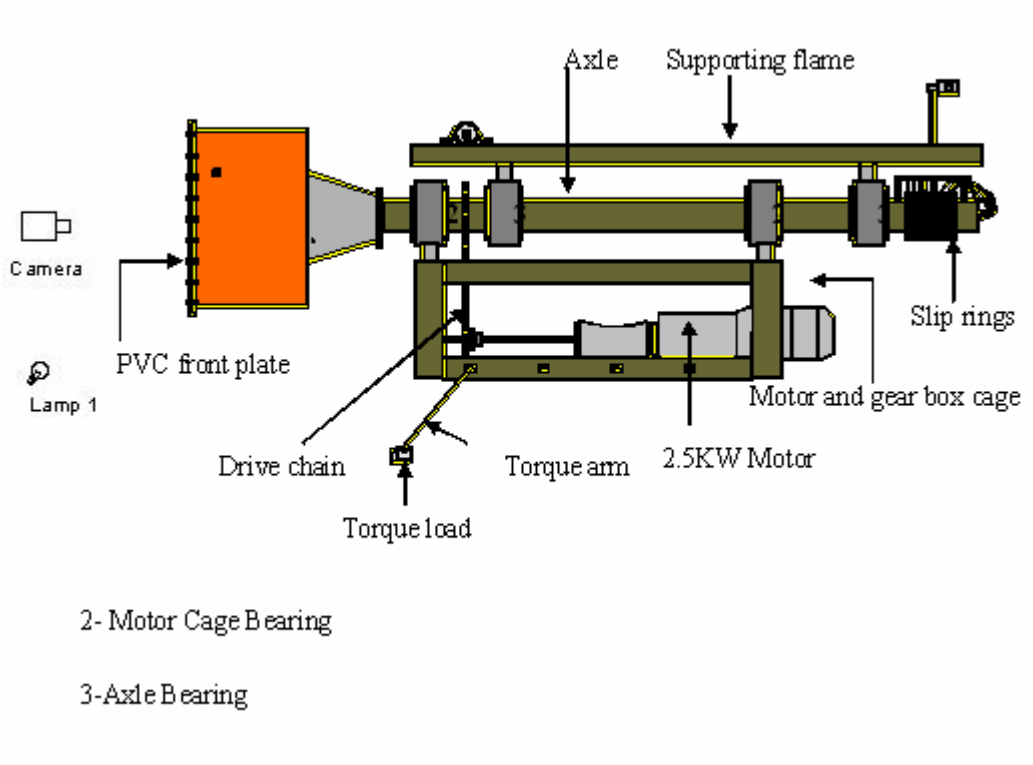

Figure 3.1: The schematic representation of the experimental mill set up

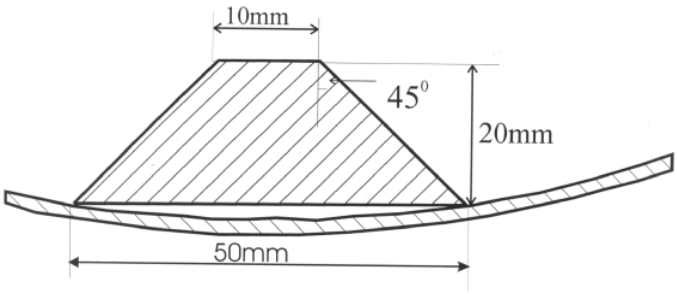

Figure 3.2: A schematic representation of the trapezoidal lifter used during the experiments.

Assuming ball and particle voidage of 0.4, the mill was initially charged with 20% ball load and 90% of the voids filled level with black powder. The mill was run at low

speed until the charge was well mixed before it was stopped. White tracer powders (10% of the particle filling level) were then introduced before it was operated at the desired speed. Tracer particles were introduced at the toe position for radial measurements while for axial experiments they were put at the back of the mill – Figure 3.5. In order to ensure that the whole process is captured, video recording was started ahead of the mill being turned on. The mill was operated at the desired speed until the mixture (charge) was observed to be completely mixed.

3.1.2 Data Transfer and Analysis

The recorded video was transferred onto the Personal Computer (PC) for analysis by using Unlead VideoStudio software. This is an interactive video editing software that can be used to manipulate home videos. The video was first split into individual frames using Bink and Smacker software before analysis. In order to utilize the information from the images, a programme was written in Matlab version 13 with Image Processing Toolbox (Appendix 2).

The method adopted in data analysis was based on the fact that the amount of light reflected by the surface can be used to determine the concentration of the mixture. The video was first split into frames and converted into Gray scale before they were analysed using image analysis. It should be noted that there was no loss of data during the conversion from colour to gray scale. It was however easier to work with gray value scale because only one value is obtained rather than three different values when the RGB scale for colour analysis is used. Measurements (16*16 pixles^2) were carried out on selected parts of the charge as shown in the fig 3.3. The reflected light was measured in Gray value intensity (mean Gray value-mgv) whose scale of measurements varied from 0 to 255. This scale was therefore used to define the degree of whiteness, 255, and blackness, 0. The local composition from any point in the charge was thus measured for each of these areas by computing the mean Gray value of the pixels.

3.1.3 Image Processing

Definition:

Image processing is the computer manipulation of the images to obtain the desired results. The goal of this manipulation can be divided into three sections:

(i) Image processing: *image in – image out*

(ii) Image analysis: *image in – measurements out*

(iii) Image understanding: *image in – high-level description out*

An image may be considered to contain sub-images sometimes referred to as *regions-of-interest*, *ROIs*, or simply *regions*. Thus in most analyses, measurements are carried out on regions of interest.

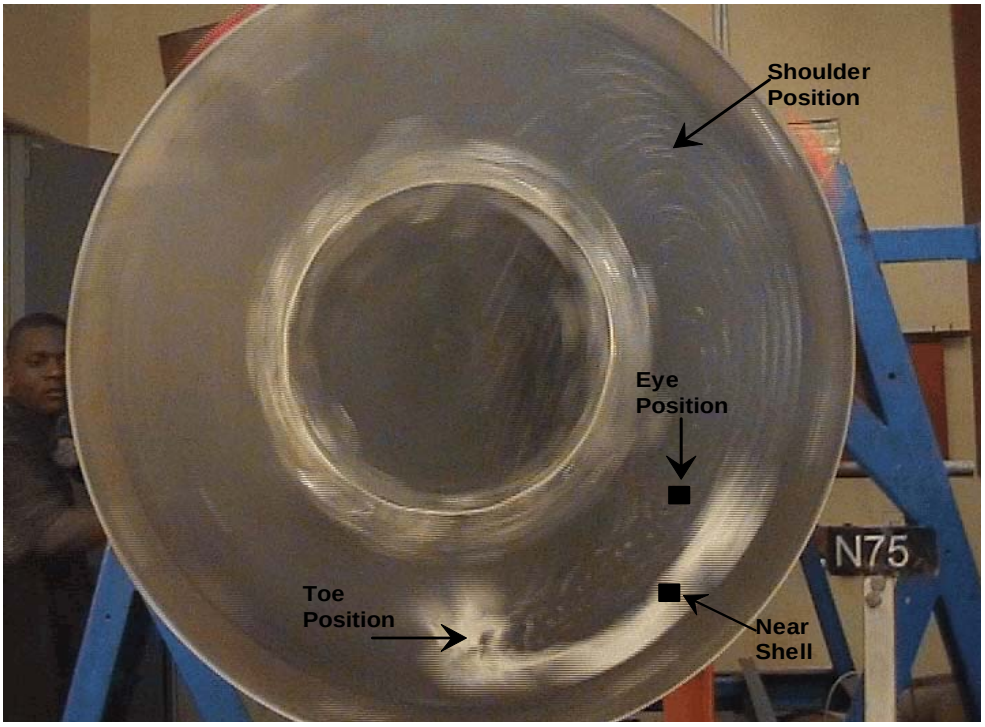

Figure 3.3: The front view of the mill charge showing the different points where measurements were performed.

3.1.4 Determination of the calibration curve

Conversion of light intensity measurements into concentration values required a calibration curve. Such a curve was obtained from a set of homogeneously mixed samples covering a wide concentration range. This was achieved by mixing known masses of powders in the mill until the mixture was homogeneously mixed. The mean gray value which corresponds to the known concentration of a particular mixture was measured. The mean gray value intensity of the region of interest obtained from one frame was the same as the mean value obtained from multiple frames. This was used as a confirmation that the charge was well mixed. A calibration curve was thus established by plotting the known concentration of the mixture against the measured mean gray values.

A typical calibration curve is shown in figure 3.4 for a system of 300μm white and black PVC plastic powders using 256 gray levels.

The concentration profile of the bed charge is closely represented by a quadratic fit. Due to the difference in the amount of light reflected from the Perspex surface as the mill rotates, different calibration curves were established for different parts of the charge. For the calibration curve below, white particles were used as tracer particles with black particles being in bulk.

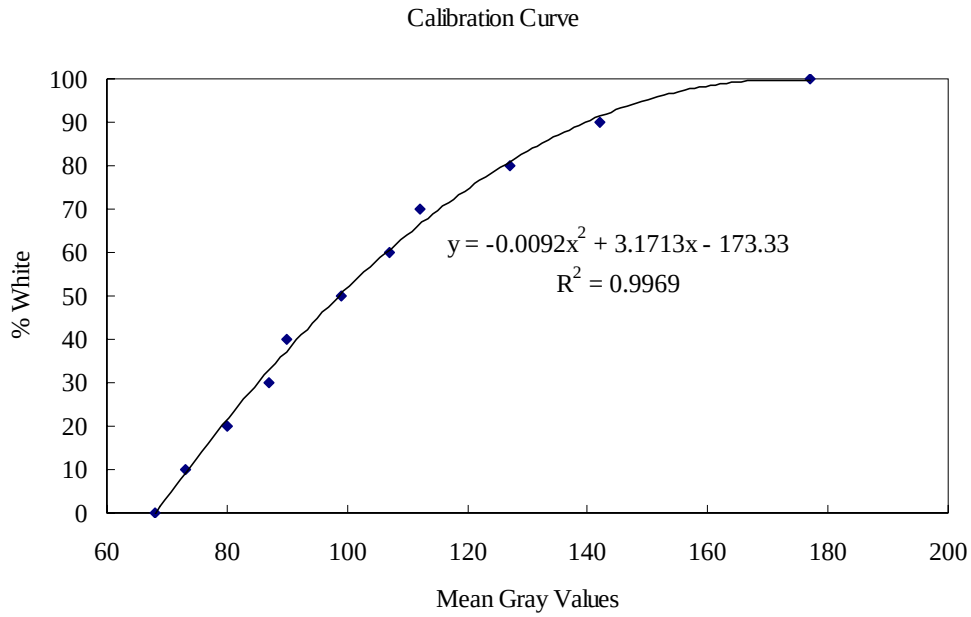

Figure 3.4: Calibration curve for the concentration (wt %) of tracer particles against gray level intensity. Each data point represents an average mean gray value of 12 frames analysed.

3.1.5 Mixing Index

In order to qualitatively and quantitatively describe the mixing process at a point, a mixing index, *I*, was established to measure the degree of mixedness.

If the measured mean gray value at a given point corresponds to concentration *c* and defining c_o as the concentration of a homogeneous mixture at the same point then

$$I = \frac{c}{c_o}$$ For I >1, then tracers in excess

=1, homogeneously mixed

<1, then tracers in deficit

Thus the adopted index is similar to section 1 of selection criteria, (Fan *et* al 1970), for binary mixtures based on statistical approach.

3.2 Experimental Procedure 2

3.2.1 Axial Mixing and Particle Distribution

Because the method described to measure axial mixing of particles above does not give detailed behaviour of particles along the mill, another method was devised to measure mixing and particle distribution along the axis of the mill.

Experiments were conducted in the same laboratory mill described in 3.1.1. The mill was conceptually divided into four equal sections from which the sample was analysed-Figure 3.5. Two charge systems were used in these experiments, i.e. steel balls – quartz and marbles – quartz. There was negligible size reduction in the marbles-quartz charge system relative to the steel balls – quartz charge system. Salt (sodium chloride) was used as tracer particles for experiments in which concentration profile was measured along the axis of the mill.

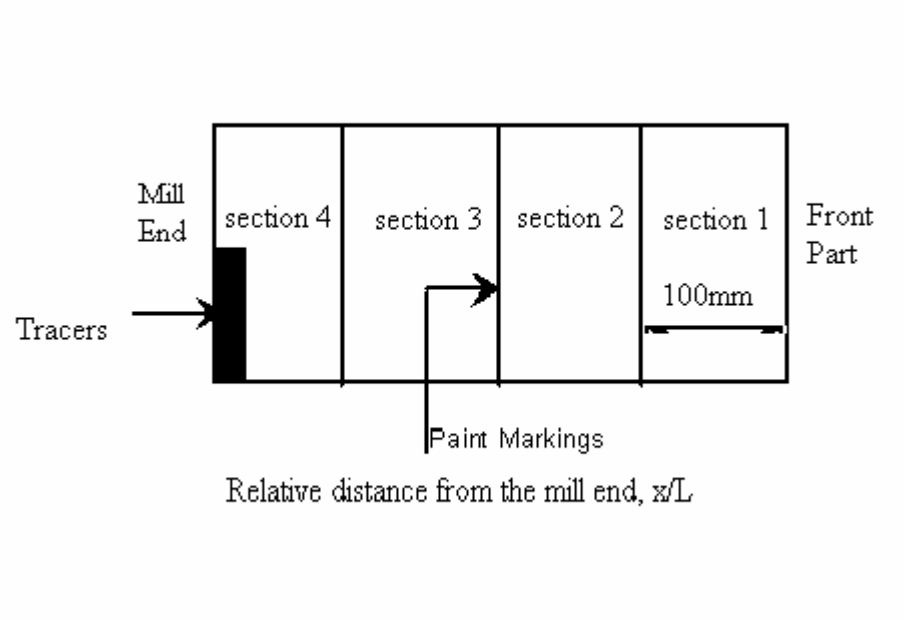

Figure 3.5 Longitudinal section of the laboratory ball mill showing the divisions. Paint was used to mark the section boundaries. The mill contents were divided into sections whose contents were analysed.

The mill was operated at 75% of the critical speed for the desired mixing time before it was stopped. After the mill was stopped, the contents were divided into 4 sections using flat steel plates that were inserted at the marked boundaries. The contents were carefully removed and collected in separate containers. The grinding media (steel balls/marbles) were later separated from the particles with the help of appropriate sieves. The masses were determined gravimetrically. The data defining the conditions of the experiments is given in Table 3.1.

Table 3.1: Experimental conditions used to determine particle distribution along the mill.

Grinding Media	**Particles**	**Mill Speed**	**Mixing Time (s)**	**% J**	**U**
Steel Balls	Quartz	75 % critical	240, 360	20	1
Marbles	Quartz	75 % critical	30, 60, 240, 360	20	1

In the determination of tracer concentration, a representative sample for analysis was obtained from the section's powder. The sample was dispersed in water and the mixture stirred continuously with the use of a magnetic stirrer. In order to increase the solubility of salt in the solution, the mixture was heated. After continuous stirring and heating, the mixture was filtered on a filter paper. The residue (quartz) was thoroughly washed with tap water to ensure that all the salt was removed. The washed residue was dried for at least 3hrs in the oven to evaporate water and the sample was weighed. The difference in masses of the sample before washing and after drying gave the amount of salt contained in the sample. This information enabled the calculation of the average salt concentration contained in each section of the mill.

The success of the above method was based on the assumption that only salt in the mixture dissolves and that no component in the quartz sublimates during drying.

3.3 Problems Encountered

(1) It was observed during experiments that particles were sticking onto Perspex front cover and steel balls after the mill was operated for some time. This may be due to the rubbing action between the balls and plastic powders leading into charge formation on the surfaces of the particles. This resulted in the attraction of particles with different charge leading to particles sticking. In order to reduce the above problem staticide solution was used. Staticide is an alcohol based anti-static solution that is sprayed on the surfaces that are affected by static electricity. The use of staticide spray eliminated the above problem.

(2) In the experimental determination of axial mixing, particles were observed to move away from the mill's front cover. This strange behaviour was investigated and results are discussed in chapter 6.

3.4 Conclusion

Experimental programs described in this work were successfully used to measure and quantify mixing and distribution of particles in a batch ball mill. The experimental program 1 enabled the continuous measurements of mixing rate without stopping the mill. The disadvantage with method 1 is that it does not give detailed information on mixing along the axis of the mill. The data analysed was obtained from measurements taken from the mill's end wall. Experimental program 2 was used to study the detailed particle distribution and axial mixing under varying milling conditions.

Valuable information that has increased the understanding on particle mixing and distribution in a batch ball mill was obtained using the experimental programs discussed above.

CHAPTER 4

Radial Mixing of Particles in a Batch Ball Mill

4.1 Introduction

Mixing of particles (ore) with the grinding media is an important aspect of milling kinetics because it affects liner wear and production rate in ball mills.

Video capture method offers a way of measuring mixing kinetics continuously without loss of data during experiments. Data obtained from the video captured has been used to measure and quantify mixing rates in a laboratory ball mill.

In this chapter, particle mixing as affected by the mill speed in ball mills is measured. A simplified derived mathematical model was successfully used to predict radial mixing kinetics. The capabilities of Discrete Element Method (DEM) to predict mixing in ball mill are also explored.

4.2 Measurements of radial mixing

Radial mixing experiments were carried out as outlined in section 3.1.1 of the experimental procedure 1 of this thesis. A series of experimental runs were conducted to investigate the effect of ball mill speed on radial mixing. For each set of experiment carried out, normalized dimensionless tracer concentration was determined with respect to time from the frames. Measurements of tracer concentration were done at selected parts of the charge as shown in figure 3.3. The mixing process was said to be complete if the tracer concentration remained constant with respect to time, otherwise more frames were analyzed.

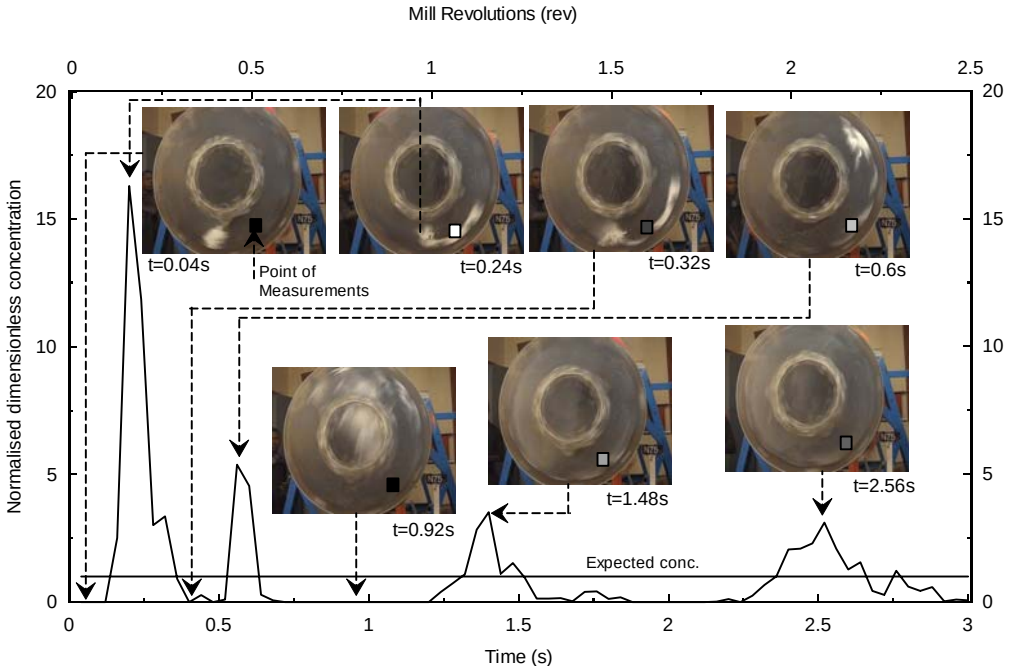

Figure 4.1, A plot of raw data points showing the first 3seconds of particle mixing measured near the shell for a mill operated at N_c=75%, ball load, J=0.2, and particle filling of U=1.0.

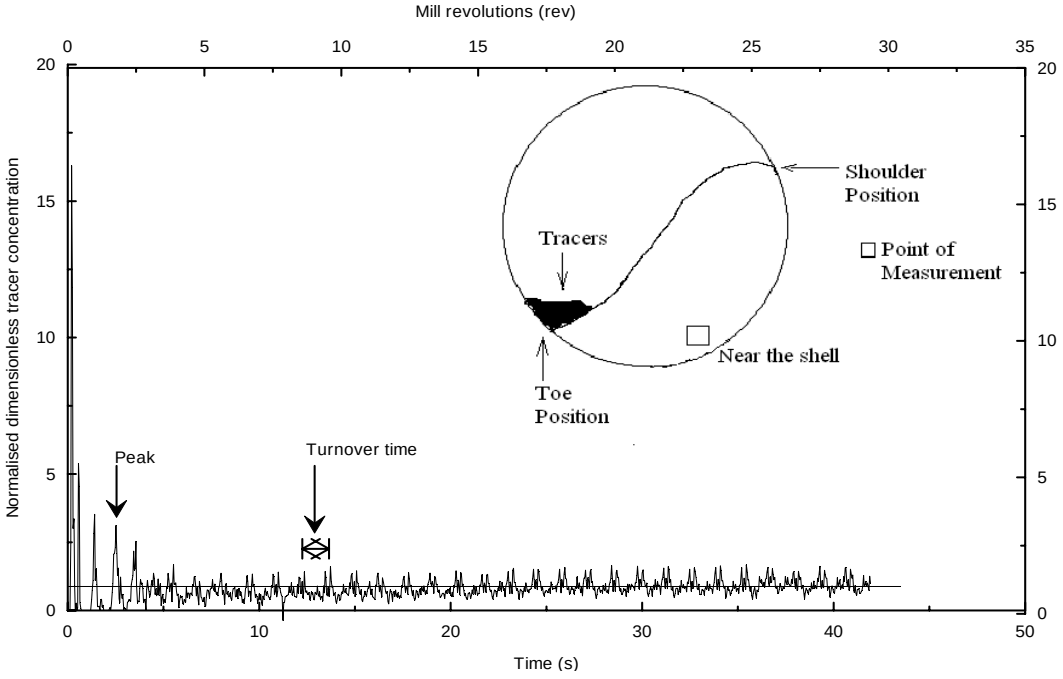

Figure 4.2, A plot of raw data points for the mixing of tracer particles measured near the shell for a mill operated at N_c=75%, ball load, J=0.2, and particle filling of U=1.0.

4.3 Mechanism of mixing

At speeds under which the experiments were conducted, particles in the charge may be divided into three distinct regions i.e. active, passive and cataracting regions. In the active region particles move from the shoulder position of the charge to the toe position, there is relative motion between the particles in this layer and the mill. In the passive region, the charge is locked together and there is little movement relative to each other. There are some particles that become air borne as they descend from the shoulder position to the toe position. These particles are said to be cataracting. The void fraction in the active region is greater than in the passive region due to the continuous relative motion of particles.

Figure 4.1 was used to describe the mixing behaviour of particles in a batch ball mill; pictures obtained from the video are also inserted in the figure. For each set of experiments conducted, normalised dimensionless tracer concentration was determined with respect to time. The figure shows that at the point of measurement, the tracer concentration was initially zero before it sharply increased to a maximum at t=0.24 seconds. The concentration briefly dropped to zero within a fraction of a second before going up again slightly after 0.1seconds. The concentration dropped and remained at zero for half a second before going up again. The process was repeated and mixing of tracer particles was observed to occur as a series of consecutive concentration peaks. The graph also shows that the concentration peak heights decreased as mixing proceeded. Mixing of particles was said to be complete when there was no observed change in concentration peak heights with time.

The concentration was initially zero at the beginning because the tracers were introduced at the toe position of the charge (insert at t=0.04s). When the mill was switched on, the tracers moved as a solid mass up to the shoulder position through the point of measurement. The increase in tracer concentration therefore corresponds to the point when the point of measurement was occupied with tracer particles only. The concentration briefly dropped to zero because the tracers were replaced by the black

particles as mill rotation continued. The brief drop in tracer concentration was due to the way the tracers taken up into the charge during rotation. Photographs at t=0.32s and t=0.6s show that some tracers remained behind causing a break from others as they entered the charge when the mill was switched on. The tracer concentration dropped and remained zero for sometime because the tracers were replaced by black powders as they circulated around the mill. At the shoulder position, the tracer particles were projected into the air (cataracting stream) while other particles avalanched down the free surface (cascading stream) - photograph t=0.92s. There was redistribution of particles as they cascaded and cataracted down to the toe position. Little mixing of tracers was observed, mainly due to shear, with other particle during the solid mass movement as traces were locked into position by mill shell and liners. It was however during the random redistribution of particles that mixing was observed. At the toe position, the tracers recollected and their movement repeated. Due to the redistribution of particles, the amount of tracers that recollect at the toe position decreased. This decrease in tracers was observed from the decreasing peak heights -Figure 4.1. Because each peak corresponds to the time the tracers occupy the point of measurement, the time taken between two successive peaks was equivalent to the load turnover time. The observed turnover time was 1.08sec for the mill used in the experiments operating at 75% of critical speed with a period of rotation of T=1.4s. Figure 4.2 shows particle mixing measured near the shell after a relatively longer time of mixing. From the figure it is also observed that the charge concentration is never well mixed and it is constantly changing with time (persistent oscillation). This may be due to the variable reflection of light from the Perspex wall of the front mill.

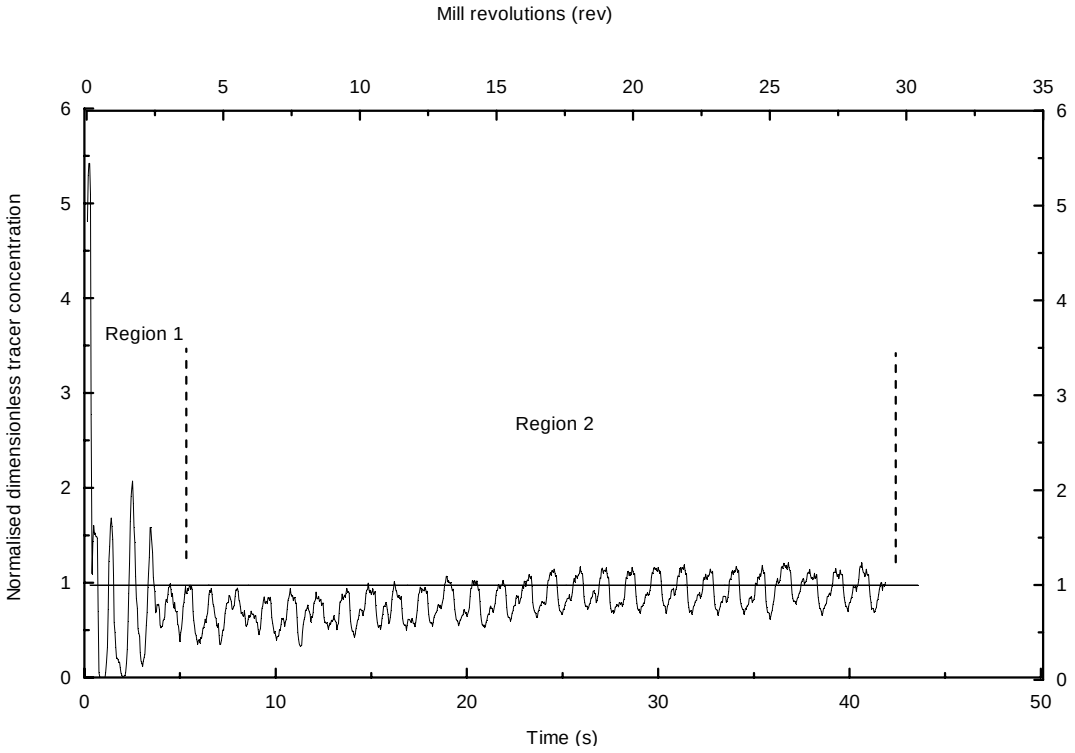

Figure 4.3, A plot of moving average data points for the mixing of tracer particles measured near the shell showing the rapid reduction in heterogeneity of the mixture for a mill operated at N_c=75%, ball load, J=0.2, and particle filling of U=1.0.

The process of mixing can be divided into two distinct regions as shown in Figure 4.3. Region 1 shows a rapid decrease in the mixture's heterogeneity (convective mixing) while region 2 represents the redistribution of particles to achieve randomness (diffusion and percolation).

Figure 4.4 represents the kinetics measured at the eye position, centre of rotation of the charge.

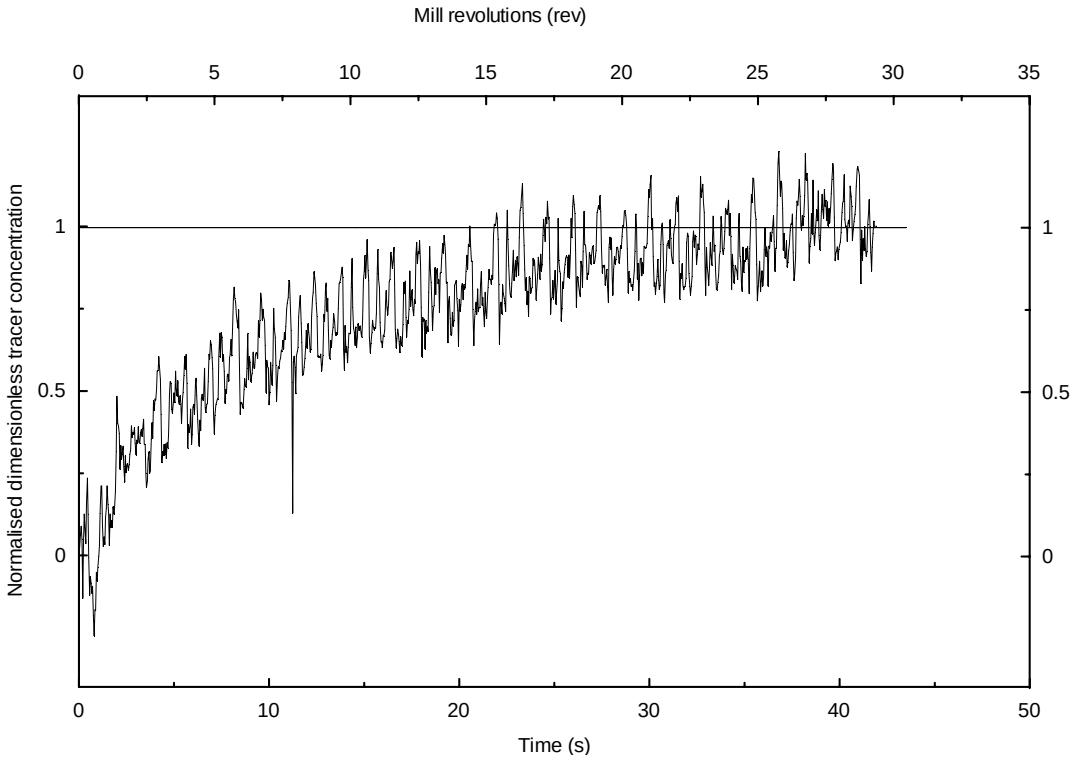

Figure 4.4, A plot of raw data points for the mixing of tracer particles measured at the eye position showing the steady increase in the tracer concentration for a mill operated at N_c=75%, ball load, J=0.2, and particle filling of U=1.0.

Figure 4.4 shows the measurements of the tracer concentration measured at the eye position. The tracer concentration starts from zero and steadily increases with time until it remained constant (if high frequency noise is ignored). The kinetics of mixing at the eye position may be explained as below:

As tracers cascade and cataract from the shoulders, they fall into the voids between steel balls of the active layer of the charge. Once in the charge, the movement of tracers was restricted to diffusion and percolation until they reached the ROI. Due to continued mill rotation, there was an influx of tracers into the charge every load turnover until the mixing process was complete.

Mixing can be affected by the speed at which a mill is operated. Figure 4.5 shows a comparison of mixing kinetics measured at the eye position as the mill speed is increased.

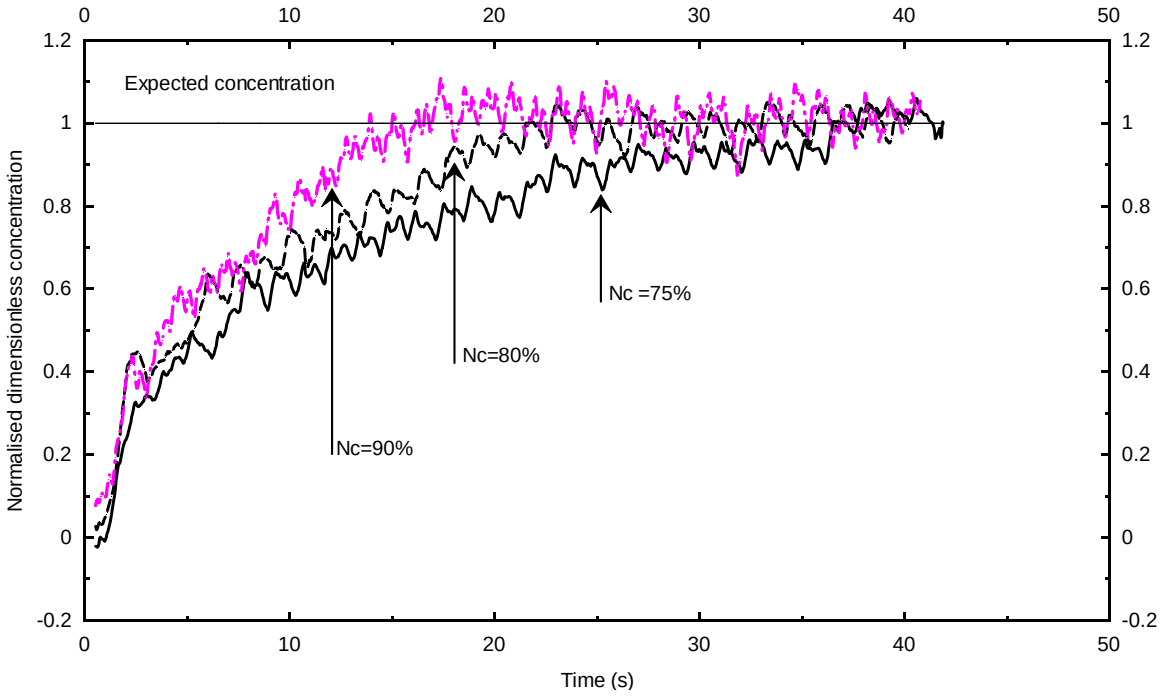

Figure 4.5, A plot of moving average data points for the mixing of tracer particles measured at the eye position showing the steady increase in the tracer concentration for a mill operated at different speeds , ball load, J=0.2, and particle filling of U=1.0.

Figure 4.5 shows the effect of speed on the rate of mixing in a dry batch ball mill. It can be observed from the figure that the rate of mixing increases with increasing mill speed. It took 9s for mixing of particles to reach 80% completion for the mill operated at Nc=90% whereas for Nc=80% and Nc=75% it took 14s and 17s respectively. This may be due to the increased amount of charge material thrown into the radial-circumferential plane of the mill per unit time as the cataracting stream increased, (Cleary 2003). It can also be noted that as the mill speed increased, the signals become noisier. This maybe due to the differences in the mixing mechanisms involved, (Santomaso *et al* 2005). At higher speeds, convection is a dominant

mechanism of mixing whereas diffusion mechanism dominates at lower speeds. This may lead to a conclusion that it is increasingly difficult to achieve randomness in a mixture at higher speeds. These results compare well with the findings of Finnie *et al* (2004) who concluded that better mixing in rotating cylinders can be achieved at lower speeds than at higher speeds.

4.4 Radial Mixing Model

4.4.1 Model Derivation

In model derivation, it was assumed that the charge is made up of two regions as shown below:

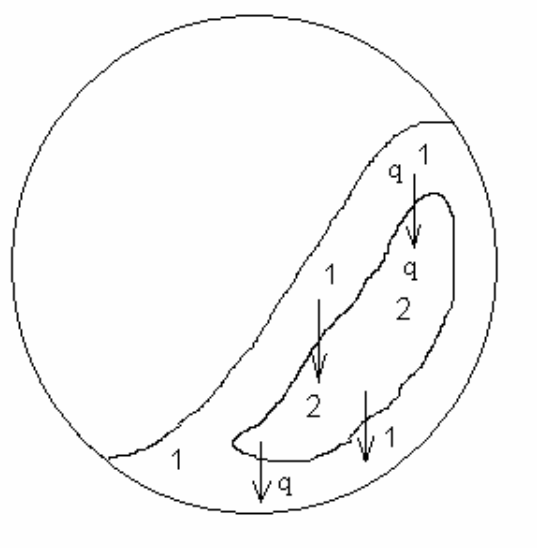

1=outer region

2=inner region

q=mass flow rate

Figure 4.6 Radial section of the mill showing the flow of material into and out of two hypothetical regions.

The process was modelled by a simplified mathematical expression based on the following assumptions:

(a) the mill charge was well mixed in both regions with different concentrations
(b) No accumulation of material in the two regions (only tracer concentration changes)
(c) Constant flow of material into and out of both regions

Applying a mass balance around region 2 we have

$$m_2 \frac{dc_2}{dt} = qc_1 - qc_2 \qquad 4.1$$

The total mass of tracers in the mill can be expressed as

$$m_1 c_1 + m_2 c_2 = m_t \qquad 4.2$$

and defining the steady state concentration as

$$\frac{m_t}{M_T} = c_o \qquad 4.3$$

substituting equations 2 and 3 into equation 1 we have

$$\frac{dc_2}{c_o - c_2} = \frac{qM_T}{m_1 m_2} dt \qquad 4.4$$

Integrating equation 4 and using boundary condition $c_2 = 0, t = 0$ and $c_2 = c, t = t$ we obtain

$$c^* = 1 - e^{-kt} \qquad 4.5$$

where $k = \frac{qM_T}{m_1 m_2}$ (s^{-1}) is a quantity that defines the rate of mixing

q = mass flow into and out of the regions (kg/s)

m_1 & m_2 = Mass of particles in regions 1 and 2 respectively (kg)

M_T = Total mass of particles in the charge (kg)

m_t =Total mass of tracers in the charge (kg)

c_o = Steady state tracer concentration (kg/s)

c_1 = Tracer concentration due to region 1 (kg/s)

c_2 = Tracer concentration due to region 2 (kg/s)

c^* =Dimensionless tracer concentration, $c^* = \frac{c}{c_o}$

4.4.2 Validation:

The model derived above was fitted to the experimental data in order to determine the rate of mixing, *k.* The figure below shows how the experimentally measured data compares with the model prediction.

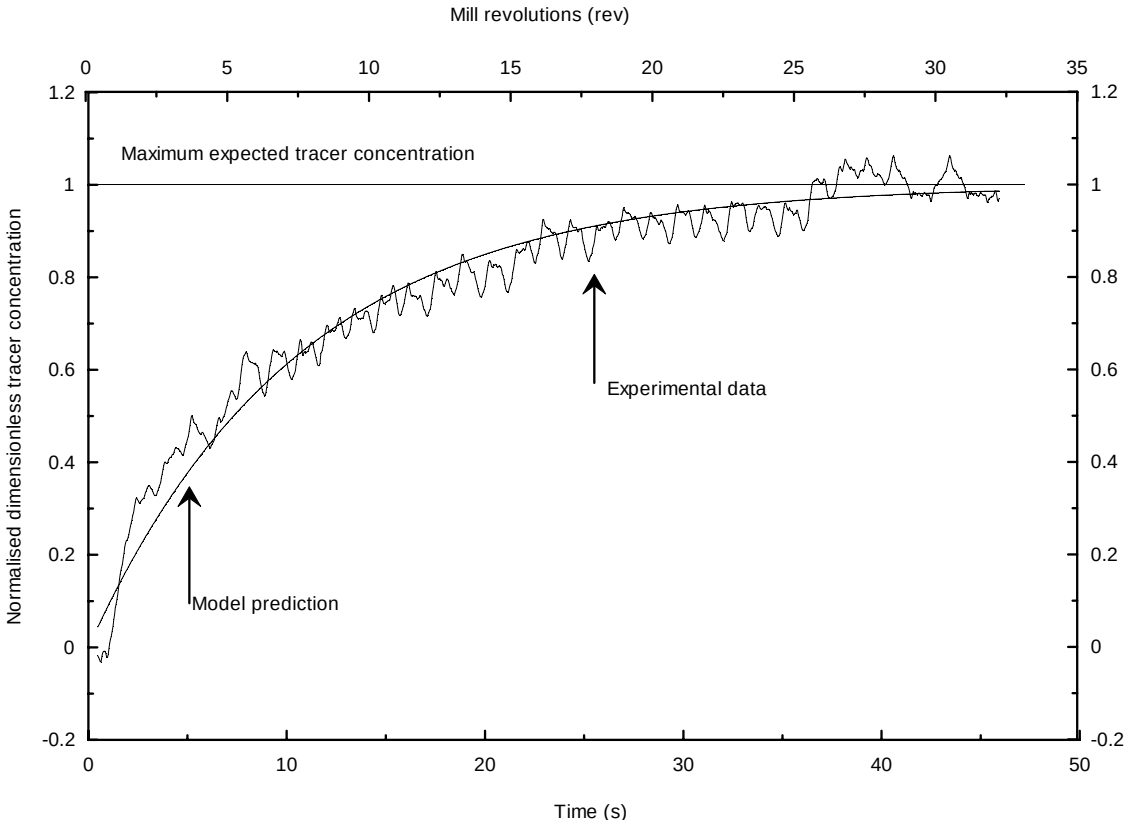

Figure 4.7 Radial mixing model was fitted with experimental data measured at the eye position of the charge giving k=0.095 (s^{-1}) at N_c=75%, J=0.2 and U=1.

The rates of mixing were determined for different mixing speeds and the dependence of k on speed was plotted and was observed to be $k \, \alpha \, N^3$, Figure 4.8.

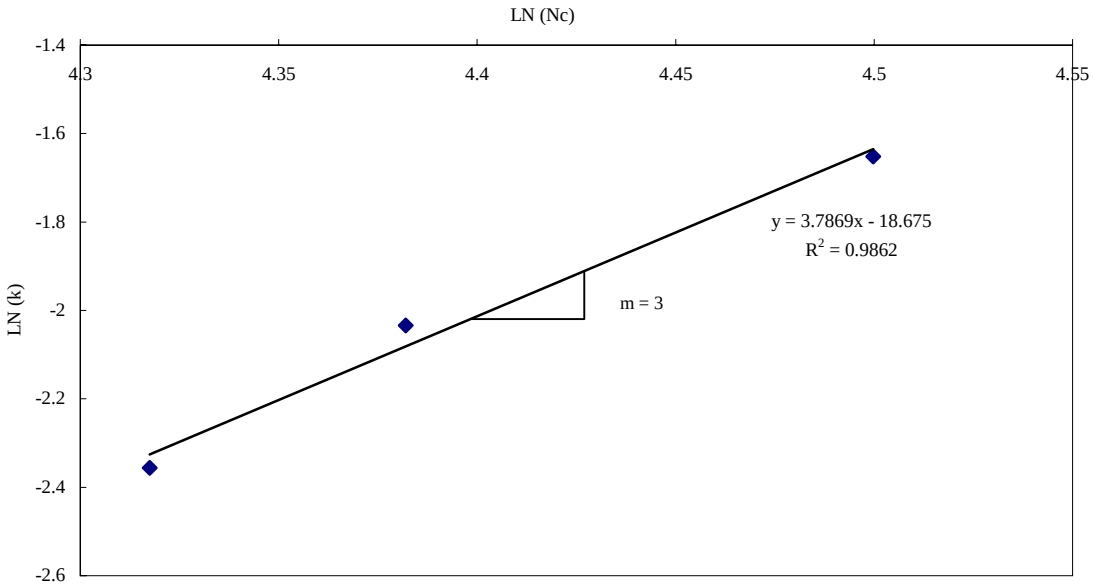

Figure 4.8 A plot of mixing kinetics with speed on a log-log scale produces a linear graph giving a slope, m, of 3.

4.5 Discrete Element Method (DEM)

This is a simulation method that has been used successfully in modelling granular flows. In this study, DEM was also used to simulate mixing kinetics and its predictions compared with experimental results.

In the DEM simulation, the mixing pattern in a 540mm diameter by 62mm length mill loaded to 20% of its volume was examined. The mill's speed was set at 75% of critical, loaded with steel balls of different diameters. 5mm and 20mm diameter steel balls were used in order to differentiate the grinding media from the particles. The big balls simulated the grinding media while small balls simulated particles. The parameters used were $\varepsilon_{b-b} = \varepsilon_{b-w} = 0.9$, $\mu_{b-w} = 0.4$, $\mu_{b-b} = 0.14$, and the $\frac{k_s}{k_n} = 0.75$. A total of 10,314 particles were used in the simulation taking 7 weeks of

computer time for a revolution. Because only one revolution was simulated, a program in Matlab (see appendix1) was written to extend the number of revolutions to any desired number. This was necessary in order to save on time.

4.5.1 Measuring mixing using DEM

(1) All balls and particles in the simulation were numbered, each ball was identified by its unique number.
(2) Particles were differentiated from grinding media in the simulation program by using different densities and sizes.
(3) Tracer particles were defined based on their distance from the origin in the first frame. Particles near to the toe position were marked as tracers.
(4) A region was defined where measurements were carried out. This region was called a region of interest (roi).
(5) Suitable measurements were chosen for the region of interest that was placed over a flow domain.
(6) Particles contained in the region of interest were counted from which the number of tracers was also determined
(7) A fraction of tracers, *c,* contained in the region of interest was determined.
(8) A mixing index, dimensionless concentration, was estimated and given by:

$$c^* = \frac{c}{c_o}$$

Data collected from DEM predictions was plotted and compared with experimental data. The results are presented in the figures below

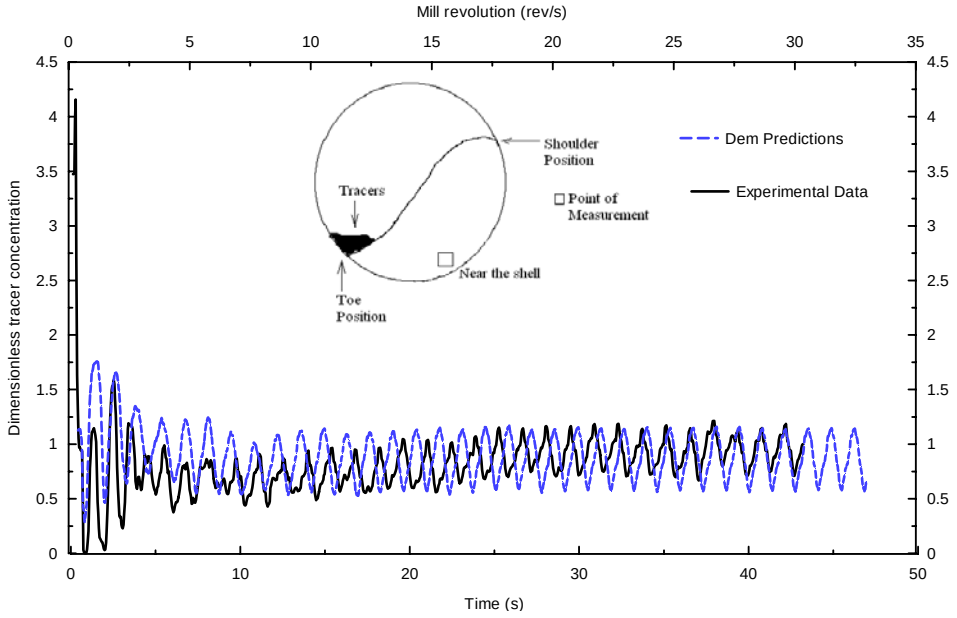

Figure 4.9 A comparison plot for experimental and DEM predictions for the mixing of tracer particles in mill operated at N_c=75%, ball load, J=0.2, and particle filling of U=1.0 (moving average data points).

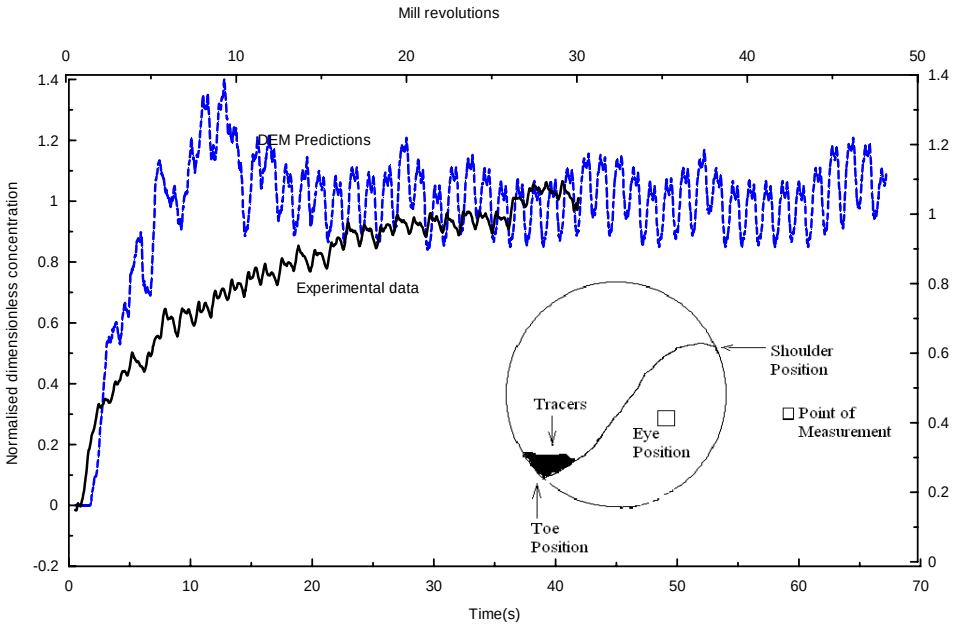

Figure 4.10, A comparison plot for experimental and DEM predictions for the mixing of tracer particles in mill operated at N_c=75%, ball load, J=0.2, and particle filling of U=1.0 measured at the eye position.

The figures above show the comparison of DEM predictions with experimental data measured at different positions of the charge. Mixing of particles occurs as a series of consecutive peaks until the final bed concentration is attained. The charge turnover time for the DEM simulations was 1.1 sec compared to the experimental time of 1.08sec. The above figures, 4.8 and 4.9, show that DEM predicts particle mixing to be much faster than experimental data. For measurements near the shell, DEM simulations show that particle mixing was complete after 5 revolutions whereas it took 15 mill revolutions for experimental mixing to reach completion.

The DEM results presented above show deviation from the experimental results, this may be due to the following reasons:

(1) The mill charge used in the experimental set up was different from the charge used in the DEM set up. This affected the overall behaviour of the charge.
(2) 1:4 particle to grinding media size ratio was used in the simulation as compared to 1:330 in experiments.
(3) The mill length used in the simulations was shorter than the length for the laboratory experiments. A 3 ball diameter mill length was used for the simulations while a 10 ball diameter length was used during experiments.
(4) The parameters used in the simulation were not determined based on experimental conditions.
(5) The mixing process in the simulator may also have been affected by the end wall effects due to the shear forces. The effect of the shear forces in the simulator are expected to be higher because of the short mill length used.

4.6 Conclusions

A Video capture method has been used to measure radial mixing in a ball mill from the end wall. The results of this work were not affected by the fact that the method used does not give detailed information on mixing along the mill. This was justified by the use of the short mill length so that axial mixing of particles could be neglected.

Radial mixing of particles is a fast process taking less than 25 revolutions to reach completion at mill speeds and length used. It is difficult to achieve a random mixture at higher speeds though the rate of mixing increases with increasing speed. A simple mathematical model has been derived that could be used to predict radial mixing in a ball mill.

The capability of DEM to simulate the mixing process has also been explored. For comparison purpose, it is required that parameters used in DEM simulations be determined based on the experimental set up.

CHAPTER 5

Axial Mixing of Particles in a Batch Ball Mill

5.1 Introduction

Axial mixing experiments have mainly been studied using the concept of residence time distribution, (Gardener *et al* 1980). Due to the harsh working environment, studies on ball mills rely on observation of the products from the feed material while treating the ball mill itself as a black box. The determination of residence time distribution of particles in ball mills is mainly achieved by measuring the tracer concentration at the mill exit that has been introduced into the mill at the feed point.

Austin *et al* (1983) fitted the axial mixing model to the experimental measurements from radioactive tracer tests to determine the particle residence time distribution in a laboratory and pilot mill. Martin (2003) measured the axial mixing of the slurry in an industrial wet mill using the salt tests. The ability of Discrete Element Method to predict mixing of particles in ball mils was also explored. Cleary (2003) used the three dimensional DEM to simulate the axial mixing and particle transport of particles in a mill.

This chapter presents the results of axial mixing experiments measured from a laboratory batch ball mill from two experimental methods. Continuous measurements of axial mixing kinetics in a batch mill were obtained by capturing the process on a video camera from the end wall in method 1. The second method involved the conceptually dividing of the ball mill into 4 equal sections. After mixing, the samples from the sections were analysed for the tracer presence. Unlike method 1, measurements in method 2 were only obtained after a defined mixing time.

5.2 Axial mixing model

The batch axial mixing model for a reactor is defined as

$$\frac{\partial c}{\partial t} = D\frac{\partial^2 c}{\partial z^2} \qquad 5.1$$

where c is tracer concentration (gram tracer per gram solid) at time t, D is diffusion coefficient (m^2/s) and z is the axial distance from the mill's feed point.

Defining boundary conditions as

(i) $c(z,0) = 0, \qquad h < z < L$

$$c(z,0) = \delta \qquad 0 < z < h \qquad 5.1a$$

(ii) $$\left.\frac{\partial c}{\partial z}\right|_{z=0} = \left.\frac{\partial c}{\partial z}\right|_{z=L} = 0 \qquad 5.1b$$

given that there is no diffusion at both mill ends

An analytical solution for equation 5.1 with the same conditions is given by Crank (1975, pp63) as:

$$c = c_o\left\{\frac{h}{Z} + \frac{2}{\pi}\sum_{n=1}^{\infty}\frac{1}{n}\sin\frac{n\pi h}{Z}\exp(-\frac{Dn^2\pi^2 t}{Z^2})\cos\frac{nx\pi}{Z}\right\} \qquad 5.4$$

Where x is the point of measurement

5.3 Measurements of axial mixing

Axial mixing in a batch ball mill was measured using both methods described in chapter 3 of this thesis.

5.3.1 Method 1

Measurements at the end wall for the variation of tracer concentration are presented the figures 5.1 and 5.2.

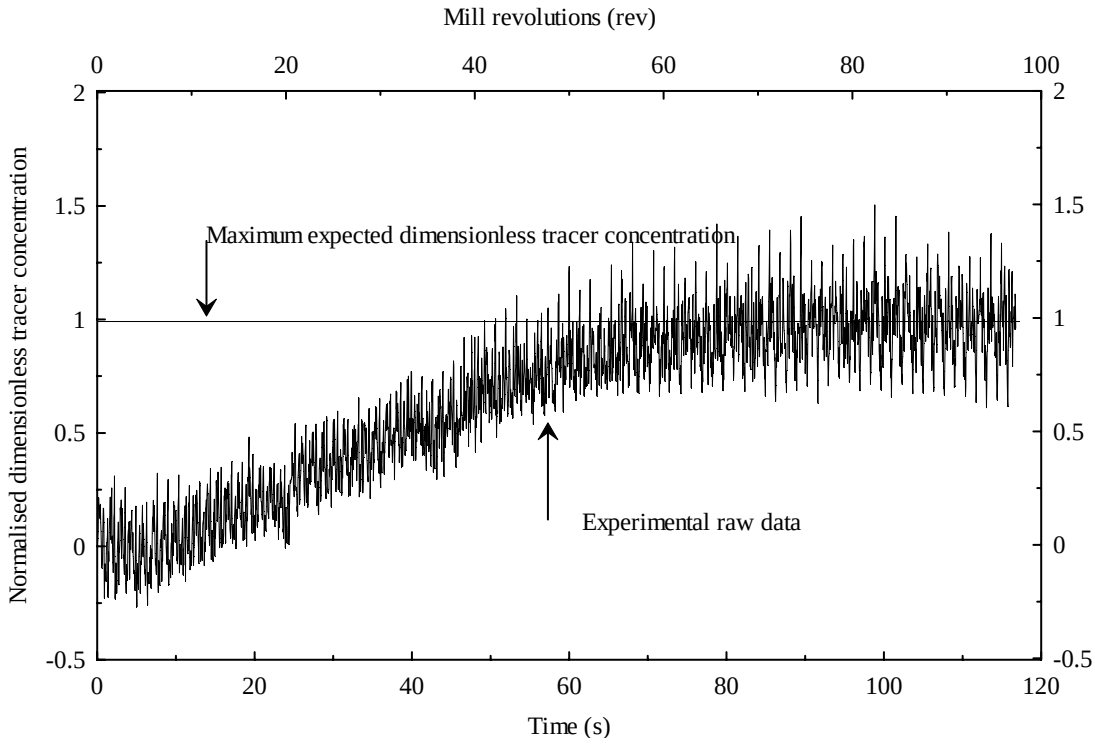

Fig 5.1 A plot of raw data obtained from the analysis of axial mixing experiments measured over a long period of mixing in the mill operated at N_c=75%, , J=0.2, and U=1.0

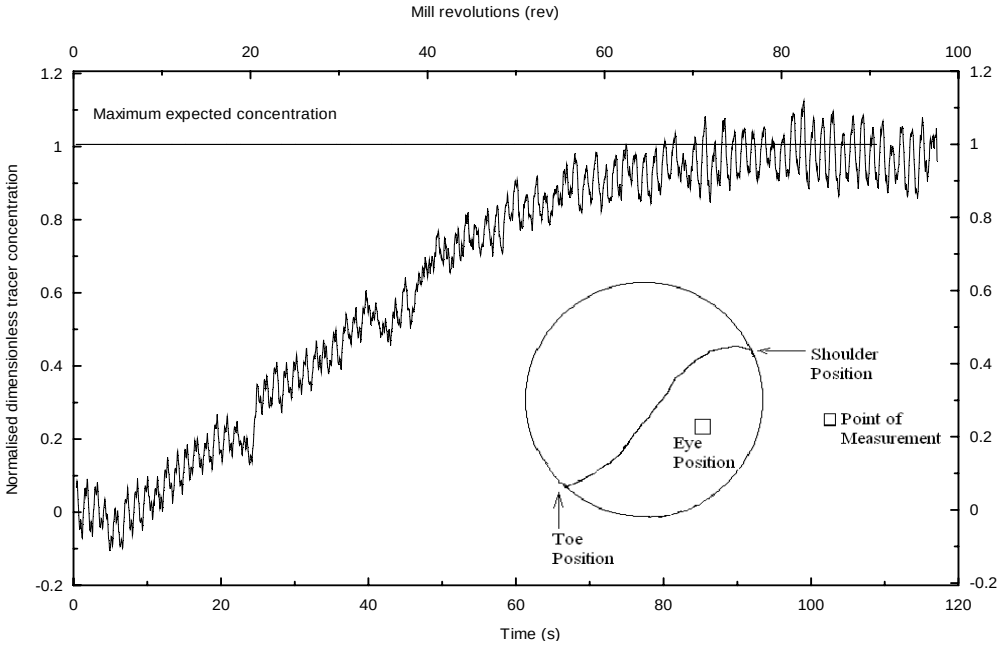

Fig 5.2 A plot of moving average data for conditions in Figure 5.1.

The figure shows that the measured tracer concentration remains zero until the 5th revolution. The tracer concentration remained zero for sometime because the tracers were introduced at the back of the mill while measurements were done on the mill's front plate. After 5 revolutions, the tracer concentration increased steadily until the 80th revolution after which the concentration remained constant an indication that the process was complete. It took a minute for mixing to reach 80% completion for the mill used in the experiments. The axial mixing process is slow and diffusion dependent as contrasted to radial mixing discussed in the previous chapter.

Particle diffusion in a mill can best be described by considering particles avalanching down the charge's free surface from the shoulder position. As the particles avalanche, they collide with other particles and their random movement is governed by their size. Thus larger particles will travel a longer axial distance than smaller particles because of the increased momentum. Secondly, the chances of smaller particles getting trapped in charge voids are higher thus restricting their movements.

The particles continue to flow until they reach the toe position of the charge. At the toe position, particles enter the passive region of the charge and move as a solid mass until they exit at the shoulder position. Their movement within the charge can be described by the mill's radial velocity governed by the bulk flow of material. There is no axial movement of particles in charge because they remain locked in position by other materials and the mill's shell and or liner. At the shoulder position, the process is repeated until the particles exit the mill.

5.3.2 Method 2

The figure below shows the results obtained from measurements of concentration profile along the mill at different mixing times.

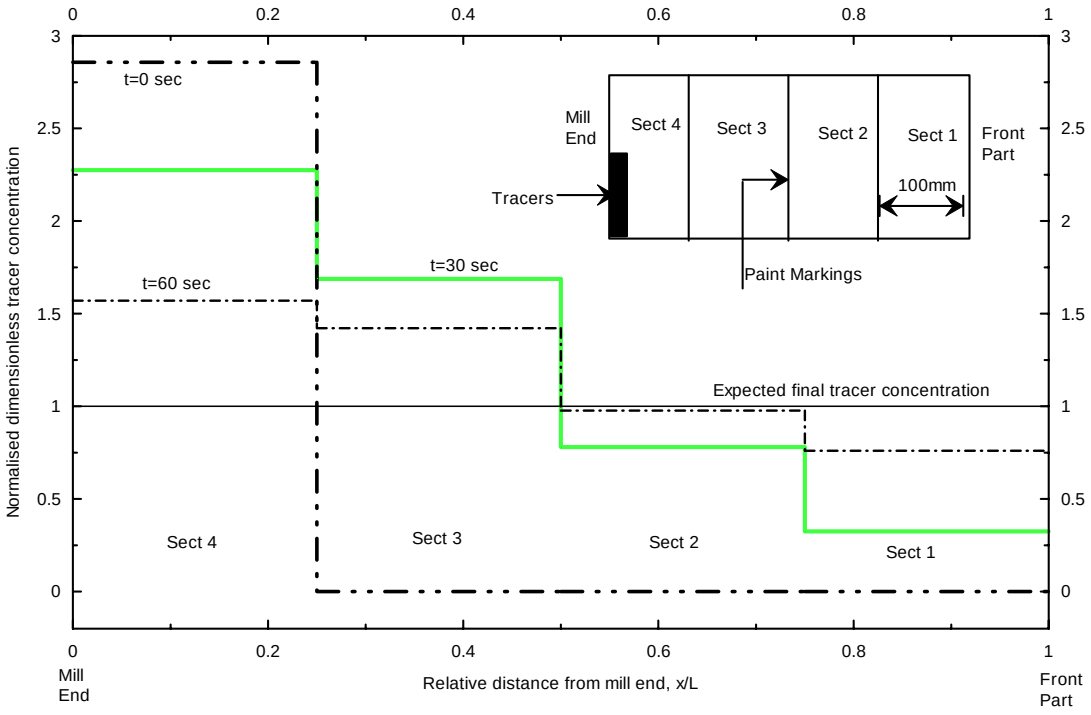

Figure 5.3: A plot of average axial tracer concentration profile obtained at different mixing times for a laboratory mill operating at Nc=75%, U=0.62 and J=0.21. Marbles and Quartz charge system was used in the experiments. The mill was divided into 4 equal sections whose contents were sampled for tracer analysis (insert).

Figure 5.4 shows the average tracer concentration profile for the marble-quartz charge system at different mixing times for each section. The figure shows that no tracer particles were present in other mill sections apart from section 4 at the beginning of the experiments, t=0. This was because the tracers were placed at the back of the mill as shown in Figure 4 insert. When the mill was switched on, due to charge dispersion, it was observed that the average concentration of the tracer particles gradually increased in mill sections 1-3 and decreased in section 4. As mixing time was increased, the mill's section tracer concentration approached a uniform value.
At infinite mixing time, the tracer concentration in the mill is expected to be the same in all the sections. Infinite mixing time as used here applies to mixing time long enough until the charge is well mixed.

5.4 Modelling of Axial Mixing

By fitting the axial mixing model to the data collected from method 1, the particle's diffusion coefficient, *D,* of 0.038–Figure 5.5.

For measurements from method 2, the determined diffusion coefficient was *D=0.029* (for 30s mixing) and *D=0.028* (for 60s mixing) respectively. The results show rapid mixing for the charge used in method 1 relative to the charge used in method 2. The difference may be attributed to the differences in particle milling rate for the two charge systems. There was negligible size reduction in the steel balls- plastic powders charge system whereas substantial milling of particles was observed in the steel balls – quartz charge system.

Shoji *et al* (1973) have concluded that mixing coefficients determined from batch experiments are lower relative to those determined from continuous experiments under the same conditions. This is due to the fact that particles have a tendency of moving towards the centre of the mill in batch experiments. Bulk movement of

particles is therefore not taken into account resulting into lower dispersion coefficients.

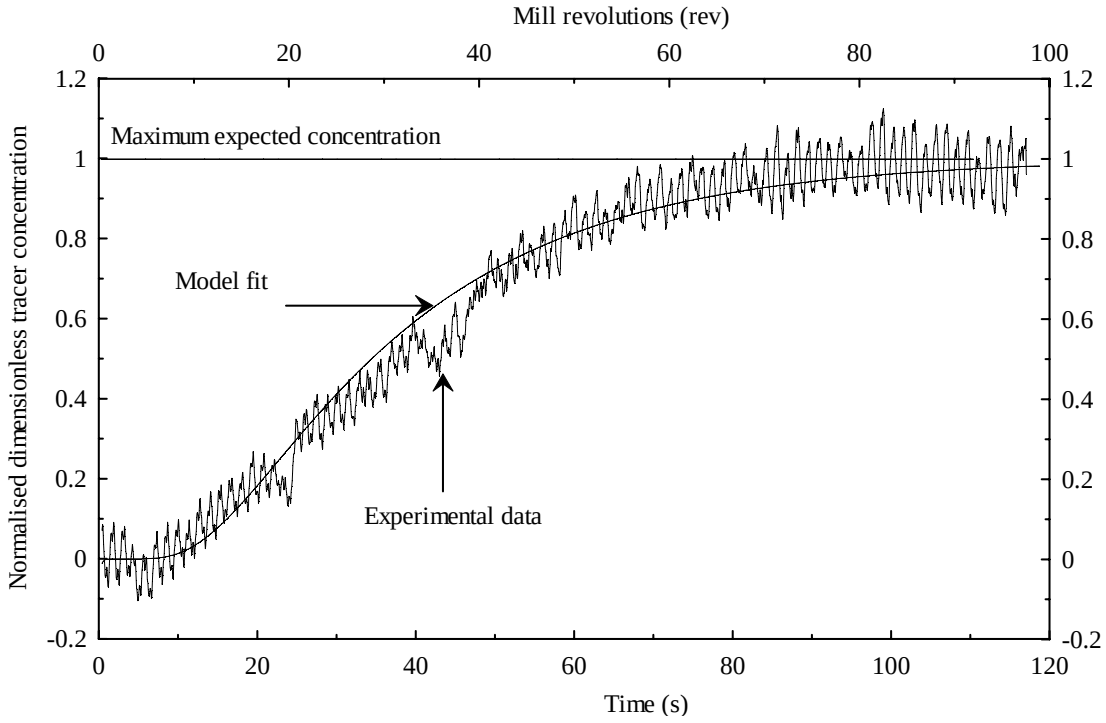

Figure 5.4 A plot of moving data obtained from the analysis of axial mixing experiments measured over a long period of mixing in mill operated at N_c=75%, ball load, J=0.2, and particle filling of U=1.0. The mixing model was fitted to the data giving the D^*=0.038

5.5 Discrete Element Method (DEM)

The capabilities of DEM to predict particle mixing in the axial direction were also investigated. The parameters used to simulate radial mixing kinetics were also used to study axial mixing. In a 0.28m long mill, 6545 particles were used in the simulation taking 3 weeks of computer time for a revolution. The same program used in chapter 4 to extend the number of revolutions was also used here.

5.5.1 Measuring mixing using DEM

The method used to quantify mixing of particles is the same as the one employed for radial mixing of section 4.5.1. The only difference was that in axial mixing the particles near the back of the mill were labelled as tracers as contrasted to particles near the toe position for radial mixing.

Data collected from DEM predictions was plotted and compared with experimental data. The results are presented in the figures below

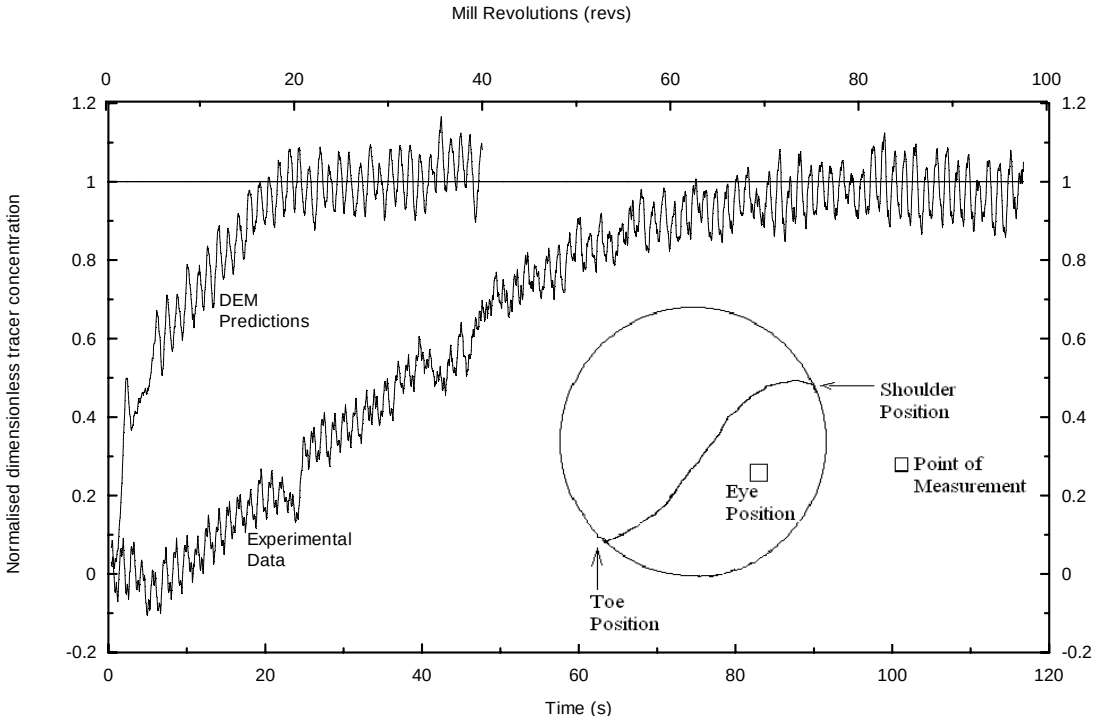

Figure 5.5, A comparison plot for experimental and DEM predictions for the axial mixing of tracer particles in mill operated at N_c=75%, ball load, J=0.2, and particle filling of U=1.0 (moving average data points).

Figure 5.4 shows the DEM predictions compared with experimental data. The results show that particle mixing was much faster in DEM predictions than experimental results. The simulation predicts that mixing of particles was completed after 20seconds while it took more than 100seconds for mixing in the experiments to reach completion.

The DEM simulation results presented in this thesis deviate from experimental data mainly because of the reasons discussed in section 4.6.2 of this thesis. Besides, a 7 ball diameter mill length was used for the simulations while a 40 ball diameter length was used during experiments.

5.6 Conclusions

Axial mixing of particles in a dry batch ball mill have been studied using two different methods. In the first approach, a video camera was used to capture the mixing kinetics from the end wall. The disadvantage of the method used above was that it does not give details of the actual mixing process along the mill. In the second method, the mill was conceptually divided into 4 equal sections and its contents sampled along the mill. Unlike the first approach where instantaneous measurements were obtained without stopping the mill, sampling of data in the second method was only possible when the mill was stopped. The accuracy of the second method was validated by performing a salt mass balance after mixing.

Axial mixing and transport of particles is a relatively slow process compared with radial particle mixing discussed in the previous chapter. A dispersion model was successfully used to quantify mixing of particles giving the particle's dispersion coefficients of $D=0.038$ and $D=0.028$ for methods 1 and 2 respectively. Mixing of particles in a batch mill was also affected by particle's tendency to segregate from the grinding media, chapter 6.

The ability of DEM to be used to measure mixing was also explored. A comparison of experimental and simulated data show a significant difference mainly because of the parameters used. The parameters were not determined based on the experimental set up. Simulation of particle mixing in ball mills was also restricted by the number of particles used in the simulation. Mill length and differences in the nature of particles used are some of the factors that affected the results. Unless a super-computer is used, the process consumes a lot of computer time (in the order of months before completion). The duration of the process depends on the number of particles, revolutions required for analysis and size of particles used in the simulation.

A detailed study of mixing demonstrates that the amount and nature of mixing is quite sensitive to the range of physical parameters-(Cleary *et al* 1998). Further work to verify the DEM capability to predict mixing should be carried out in which the above shortfalls must be addressed.

CHAPTER 6

Distribution of Particles in a Batch Ball Mill

6.1 Introduction

When conducting axial mixing experiments using the steel balls – PVC plastic powders charge system, it was observed that particles had a tendency of segregating from the balls. The particles were observed to move away from the front plate of the mill. This behaviour was also observed by Rogers and Clements (1971) and Shoji *et al* (1973).

Rogers and Clements (1971) investigated the effect of speed, particle size and density on particle segregation in a drum mixer. They reported the formation of central core and bands at the mill ends that were affected by the change in speed. The same results were obtained by Kuo *et al* (2005) in which glass beads and rubber balls were used.

Shoji *et al* (1973) investigated the distribution of particles along the mill in a batch operation. The charge comprised Silicon Carbide (bulk particles), garnet (tracer particles) and vinyl balls (grinding media) so that particle breakage was neglected. Their experimental results showed that particles formed a band at the mill centre while the grinding media was concentrated at the mill ends.

This chapter discusses the results of axial particle distribution measured along a laboratory mill charged under two different charge conditions. In the first set of experiments, the steel balls – quartz charge system was used whereas the marbles-quartz system was used in the second set. The rate of milling was higher in the first set of experiments relative to the second set of experiments after the same mixing time. This condition made it possible to study the effect of size reduction on distribution of particles in a batch ball mill.

6.2 Measurements of Particle Distribution

Experiments were carried out as outlined in section 3.2.1 of the experimental procedure 2 of this thesis. The results for the determination of particle distribution along the mill are presented below.

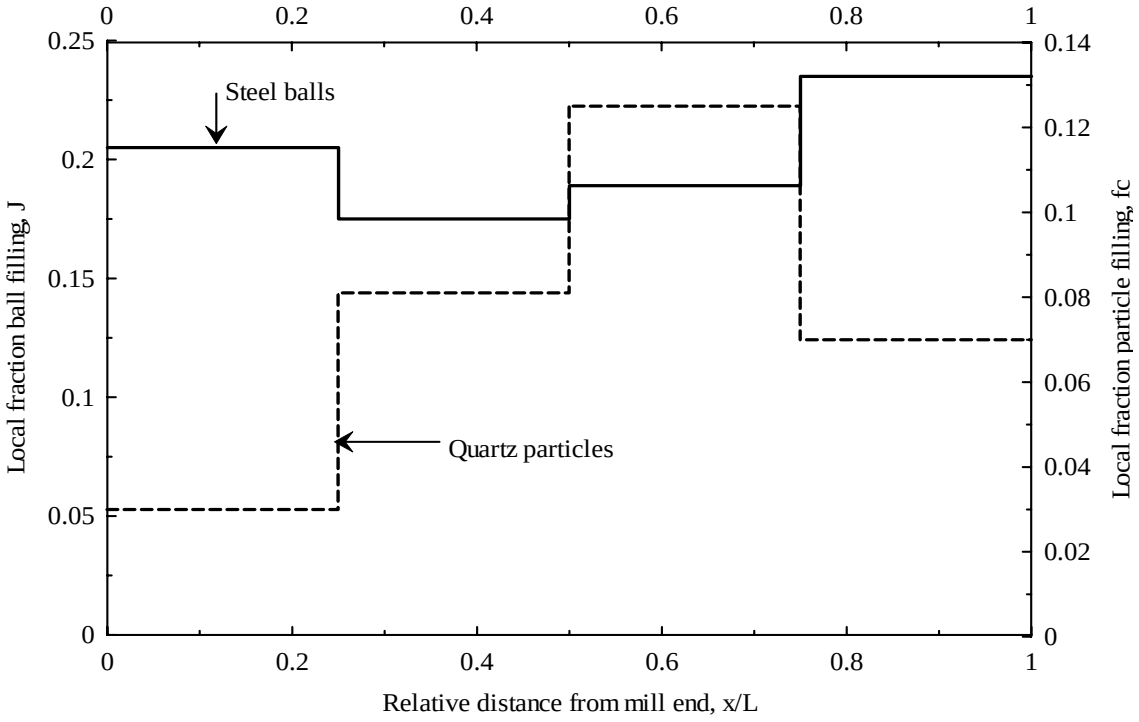

Figure 6.1 Axial distribution of particles and steel balls after 5minutes of mixing for J=0.2, f_c=0.08 and N_c= 75% showing their tendency to segregate along the mill (steel balls – quartz charge system).

The figure above shows charge distribution along the batch laboratory mill for steel balls – quartz system with appreciable size reduction. The figure shows that particles tend to segregate and form a band in the centre of the mill while steel balls had a tendency of moving to the mill ends. This behaviour may be explained as below:

Consider a well mixed charge in a ball mill that is operating at a desired speed and fill level. As the mill rotates, there is random collision of particles leading to axial movement of the charge. For a batch mill, the charge (steel balls and quartz) have an equal chance of either reporting to the centre of the mill or to the mill ends. Because there is no diffusion at both mill ends, the net flow of the charge will be from the mill ends to the centre. This may result in the accumulation of the charge near the centre of the mill. As the process proceeds, the charge at the centre of the mill will expand. Since particle transport in dry ball mills increases with increasing particle size, bigger particles (steel balls) will move more easily towards the mill ends than smaller particles (quartz). The consequence of this is that there is charge dilution at the end walls because of the reduced charge bulk density due to depletion of fines.

This behaviour of the charge may lead to a conclusion that the breakage rates in a batch mill vary along the mill axis. At the mill ends where there is low powder filling much of the energy supplied will be taken up in the steel to steel contact. This may result into low absolute breakage rates of particles and increased mill and ball wear rates.

At the centre of the mill however, the collision spaces between the balls are filled therefore higher absolute breakage rates are expected. The absolute breakage rates reach maximum when all the effective grinding zones in which collisions between tumbling balls are occurring are filled. When the section become overfilled with particles, the hold up increases but this does not increase the breakage rates as all the grinding zones are saturated. This results in reduced breakage rates due to poor ball-ball-powder nipping. There is also a problem of fine accumulation which cushions the coarse particles thus inhibiting their grinding.

This segregation due to size differences is also observed in industrial mills for continuous operations. The net flow of particles is from the feed end to the discharge end. As the size of particles reduces, their axial dispersion is also affected. In dry mills the diffusion coefficient reduces as the particle size decreases whereas the

opposite is true in wet mills. The size distribution of particles at the discharge point of a dry mill was observed by Rogovin and Hogg (1988) to be coarser than any other point in the mill. This internal classification was attributed to velocity differences of particles affected by their sizes.

This behaviour explains why dry mills are usually air swept in order to remove fines.

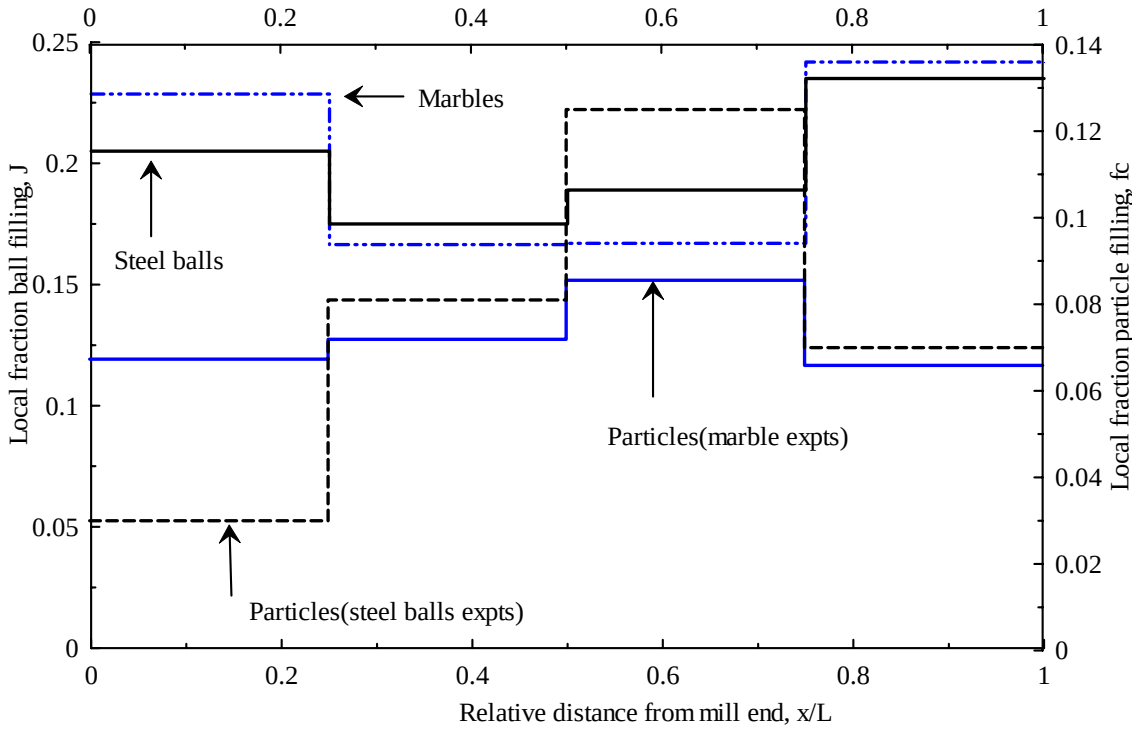

Figure 6.2: A comparison of axial distribution of particles and grinding media after 5minutes of mixing for marble – quartz system and steel balls – quartz system, J=0.2, f_c=0.08 and N_c=75%.

Figure 6.2 shows a comparison of particles and ball distribution for marble-quartz and steel balls – quartz charge system. Both systems show charge segregation with particles moving towards the centre and grinding media towards the mill ends. Particles in the marble-quartz charge are fairly uniformly distributed relative to the particles in the steel balls – quartz charge system. This may be due to the differences

in particle size in the two charge systems. The particle size in the marble-quartz system remained relatively coarser than the particles in the steel balls-quartz system after the same mixing time. This is because there was less milling taking place in the marble-quartz charge system relative to the other system. In a system where there is negligible size reduction, particles in the mill may be considered to have the same flow velocity because they have the same average size, equation 2.1. In such a system, it can be assumed that all the particles have the same dispersion coefficient and as such their distribution along the mill is expected not to vary much.

The other reason may be due to the differences in the charge density ratio of the two charge system. The charge density ratio of the system is defined as the density of grinding media to density of the particles in the system. The charge density ratio, 0.94, in the marble-quartz system is lower compared with the steel balls-quartz density ratio, 2.83. In the charge system where the particles are of the same size, the rate of segregation due to particle size increases with the increasing charge density ratio of the system. This is because the particles with higher density travel a longer distance than those with low density of the same system due to increased momentum, (Williams 1976).

6. 3 Size Distribution

In order to understand the breakage rates occurring along the mill, it was necessary to determine the size distribution of particles in each section.

To determine the size distribution, a representative sample was obtained from the section contents. The sample was wet screened to remove the -38 μm fines and dried for at least 3hrs in the oven. When the sample was dry, it was screened for 20minutes and the sample masses measured on each screen. The graphs below show the variation of size along the mill axis as a function mixing of time.

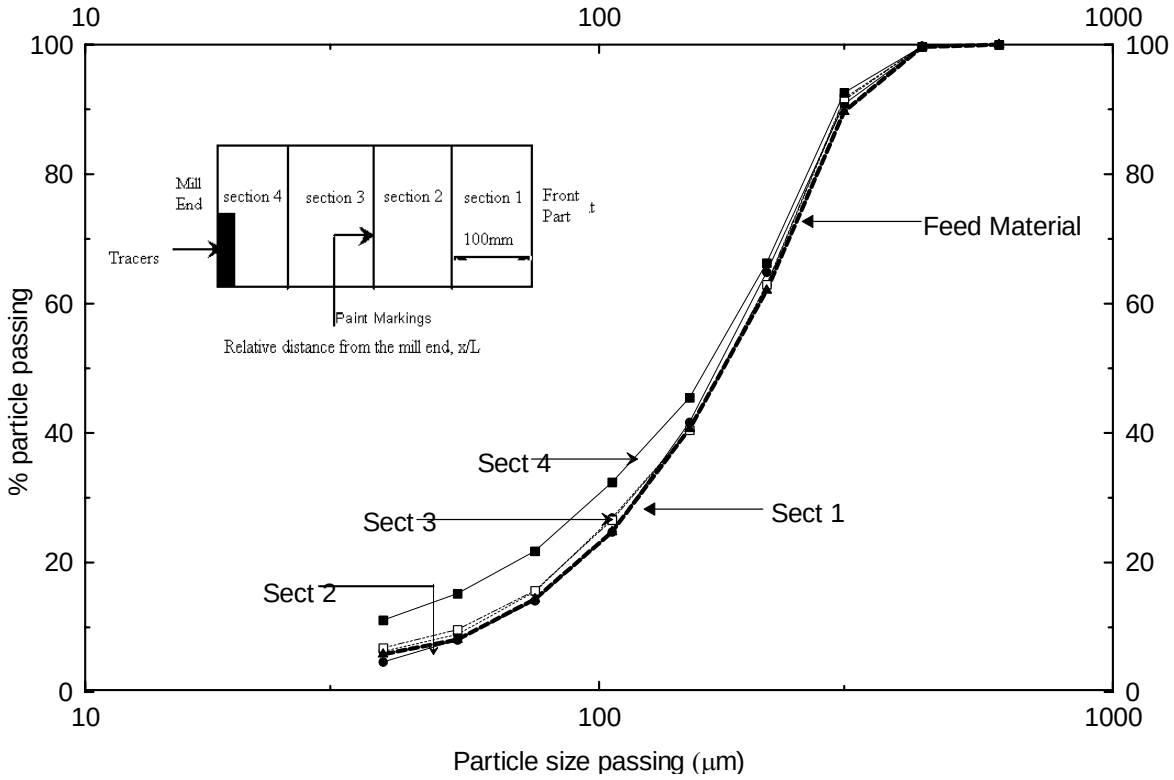

Figure 6.3: Size distribution of the particles along the mill obtained after 30 seconds of mixing time for a laboratory mill operating at Nc=75%, U=0.62 and J=0.21. Marble- Quartz charge system was used in the experiments.

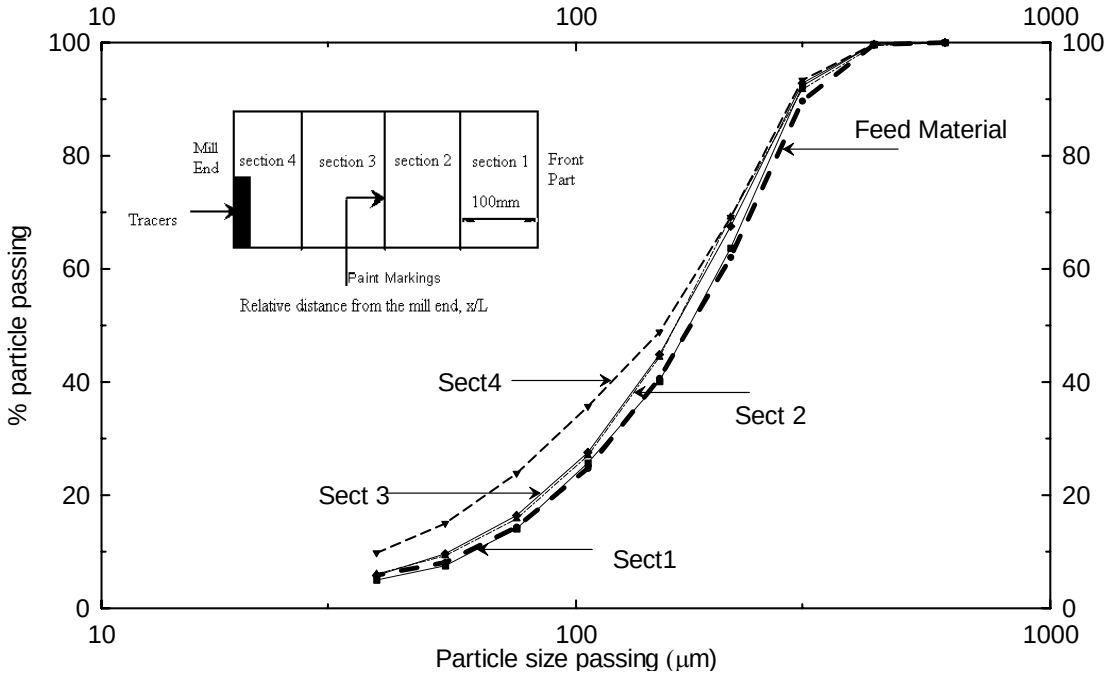

Figure 6.4: Size distribution of the particles along the mill obtained after 60 seconds of mixing time for a laboratory mill operating at Nc=75%, U=0.62 and J=0.21. Marbles and Quartz charge system was used in the experiments.

Figures (6.3 and 6.4) show the variation of particle size along the mill axis in a batch operation as mixing proceeds. Negligible particle size reduction in the Quartz- marble system was observed after 30 seconds of mixing time –Figure 6.3. The size distribution of particles in section 1, 2, and 3 was almost the same as that of the feed material. There was a significant difference in the size distribution between section 4 and other sections. The particles in section 4 were much finer relative to other mill sections. This behaviour was expected as explained above in section 6.2 of this chapter. As mixing time increases, Figure 6.4, there was a clear distinction in size distribution from section to section. It was observed that particle fineness increases from the mill front plate to the mill end.

6.4 Conclusion

Axial particle distribution along the batch ball mill was determined by conceptually dividing the mill into 4 equal sections. The method used generates some errors during separating mill's section samples for analysis (salt test). The results presented in this chapter show that the rate of particle breakage may vary from the feed point to the discharge end. The mill ends have been found to be under filled with particles thus these regions are expected to have increased steel consumption rates. The central part of the batch mill was over filled with particles a condition that could lead to reduced grinding rates. The results also showed that material near the mill end was finely ground than any other part along the mill.

There are several reasons that could lead to the uneven distribution of particles in a batch mill. The work presented in this chapter focused on the distribution of particles in a batch mill as a function of milling rate due to different charge system used. The effect of different charge bulk density and mill speed on distribution of particles in the mill opens a new area of investigation.

CHAPTER 7

Conclusions

7.1 Introduction:

This chapter presents the major findings of the work described in this thesis. It presents a summary of the work, conclusions drawn from the work conducted and recommendations.

7.2 Summary of the work

7.2.1 Experimental Procedure

Radial and Axial mixing of particles in a batch mill has been studied. In this study of mixing kinetics, a tracer technique was employed. The length of the laboratory mill was easily adjusted therefore making it possible to conduct both axial and radial experiments in the same mill. In this study, two methods of measuring particle mixing in a batch ball mill were used.

The first method employed the use of a video camera to measure mixing of particles both in radial and axial directions. In order to capture the mixing process in a ball mill, a 10mm thick transparent PVC disk was used as a mill's front plate. The main disadvantage of this method is that it does not give details of the mixing kinetics along the axis of the mill. Quantifying of particle mixing was therefore restricted to measurements obtained from the end window. Despite the above disadvantage, the method enabled the mixing to be captured continuously without stopping the mill.

The second method was only employed in measurements of axial mixing and distribution of particles. The mill was divided into 4 equal sections whose charge was sampled for analysis. Unlike the first method, this method enabled the analysis of axial distribution and mixing of particles along the mill axis though sampling could only be done when the mill was stopped.

7.2.2 Radial Mixing of Particles

Radial experiments were carried out in a 2D mill so that the axial mixing could be neglected. Radial mixing of particles in ball mill is a faster process taking 17s and 9s for mixing of particles to reach 80% completion for the mill operated at Nc=75% and Nc=90% respectively. It was observed that as the speed of the mill increased, the mixing rate increased too. The results also show that the higher the mill speed, the noisier the collected data becomes. This may be due to the increased bed voidage as the speed increased hence making it dilute with convection being the dominant mechanism. A simple mathematical model was developed that maybe used to predict the radial mixing of particles in a ball mill.

7.2.3 Axial Mixing of Particles

Axial mixing experiments were conducted in a 3D laboratory mill in which tracer particles were introduced at the back of the mill. Steel balls – PVC plastic powders charge system was used in the first method. In this charge system, there was no observed size reduction of the powders and as such the effect of milling on the process was ignored. It took a minute for mixing to reach 80% completion for a mill used in the experiments. The axial mixing model was fitted to the experimental data giving the particle dispersion coefficient of 0.038.

In the second method, a marble – quartz charge system was used to determine the axial mixing in which salt was used as tracer particles. There was measurable size reduction observed compared to the previous charge system though not as much as in the steel ball/quartz system. The Axial mixing model fitted the experimental data and the particle dispersion coefficient determined as 0,028. The calculated vessel dispersion number from the second method is lower than the value determined from the first method. This may be due to the differences in the particle size for the respective charge systems. The other reason may be due to the different charge

density ratios. There was however insufficient data collected to ascertain the effect of charge density ratio on particle distribution. Since there is more mixing a charge system where there was negligible particle breakage, it can be observed that material transport in ball mills can be affected by particle size. In dry ball mills, particle transport increases with increasing particle size.

7.2.4 Discrete Element Method Simulation of Particle Mixing

The capability of DEM to simulate the mixing process was also investigated. DEM predictions deviated significantly from the experimental results. The main reason for the differences was because the parameters used in the simulation were not determined based on the experimental set up. The mill length, size and number of particles used in simulation were also different from the experimental set up. This made it difficult to conclude on the DEM's ability to simulate mixing in ball mills.

7.2.5 Axial Distribution of Particles

Segregation of particles due to size differences was observed during the study of axial distribution of particles. Fine particles were observed to form a band at the centre of the mill while the grinding media was pushed to the mill end walls. This led to the conclusion that due to the variation in particle filling, breakage rates in a batch ball mill vary along the mill. Lower breakage rates are expected at regions near the mill ends as these sites are under filled with powders. Because of the increased steel to steel contact, higher wear rates of the grinding media are also expected near mill ends. On the contrary, high breakage rates are expected at the mill centre because of the increased encounter frequency between the grinding media and the particles (ore). If on the other hand the grinding zones there are overfilled, milling may be inhibited by the cushioning of coarse particles by fine particles.

7.5 Recommendations

More work is needed to determine particle distribution in a batch mill as affected by mill speed, charge density, effect of milling, and mill loading. Design of a safer and more accurate method to continuously measure particle distribution along the mill is necessary in order to understand the transport of particles.

In order to ascertain the DEM's potential to predict the kinetics of mixing, the parameters, $(\frac{k_s}{k_n}, \varepsilon_{b-b}, \varepsilon_{b-w}, \mu_{b-w}, \mu_{b-b})$, must be determined to simulate the experimental set up. The number of particles, mill length and the size of grinding media and particles should be the same as those used in the experimental set up.

REFERENCES

Alonso, M., Satoh, M., and Miyanam, K., 1991, “Optimum Combination of Size Ratio, density Ratio and Concentration to Minimize Free Surface Segregation”, Powder Technology, V68, pp145-152.

Austin, L. G, Klimpel, R R, Luckie, P T, 1984, “Process Engineering of Size Reduction, Ball Milling,” Society of Mining Engineers, New York.

Austin, L. G, Rogovin, Z, Rogers R S C, Trimarchi, T, 1993, “Axial mixing model applied to Bal Mills Powder Technology,” V 36, pp 119-126.

Bannister, P., and Harnby, N., 1983, Powder Technology, Powder Technology, V36, pp275.

Bridgwater, J., 1976, “Fundamentals of Powder Mixing Mechanisms”, Powder Technology, V15, pp215-236.

Brone, D., Alexander, A., and Muzzio, F., J., 1998, “Quantitative Characterisation of Mixing of Dry Powders in V-Blenders”, AIChE Journal, V44, No. 2, pp271-278.

Cahn, D. S, and Fuerstanau, D W, 1967, “Simulation of diffusional mixing of particulate solids by Monte Carlo Technique,” Powder Technology, V1 pp174-182.

Cleary, P. W, 1998 “Predicting Charge Motion, Power, Draw, Segregation and Wear in Ball Mills Using Discrete Element Method,” Minerals Engineering, V11, No 11, pp1061-1080.

Cleary, P. W, Metcalfe, G, Liftman, K., 1998, “How Well Do Discrete Element Granular Flow, Models Capture the Essentials of Mixing Processes,” Applied Mathematics Modelling, V22, pp 995-1008.

Cleary, P.W., 2003, "Axial Transport in Dry Ball Mills", 3rd International Conference on CFD in the Minerals and Process Industries, pp651-656.

Crank, J, 1975, "The Mathematics of Diffusion," 2nd Ed, Oxford Press. London.

Fan, L T, Chen, Y M and Lai, F S, 1970, Powder Technology, v61, pp225.

Finnie, G.J., Kruyt, N.P., Ye, M., Zeilstra, C., and Kuipers, J.A.M., 2005, "Longitudinal and Transverse Mixing in Rotary Kilns: A Discrete Element Method Approach", Chemical Engineering Science, V60, pp4083-4091.

Harris, C. C., and Arbiter, N., January 1982, "Grinding Mill Scale – up problems," Mining Engineering, pp 43- 46.

Heechan Cho and Austin, L.G., 2004, "A Sudy of Exit Classification Effect in Wet Ball Milling", Powder Technology, V143-144, pp204-214.

Hogg, R., Cahn, D., Healy, T., and Fuerstenau, D.W., 1966, "Diffusional Mixing in an Ideal System", Chemical Engineering Science, V21, pp1025-1038.

Kalala, J. T., and Moys, H. M., 2004, "DEM Modelling of Liner Wear in a Dry Ball Milling ", Journal of South African Institute of Mining and Metallurgy, V104, No.10, pp 597-602.

Levenspiel, O, 1972, "Chemical Reaction Engineering," 2nd Ed, John Wiley, and Sons, New York.

Mardulier, F. J and Wightman D L “efficient determination of mill retention time, Parts 1,2 and 3,” Rock Products V74, No.6 pp74-75,90-91,No 7 pp78-79, 108-110, No 8 pp60-61, 86-88.

Martin, V N, 2001, “The Characterization of Load Behaviour of an Industrial Grinding Mill” PhD Thesis, University of the Witwatersrand South Africa.

Mc Carthy, J J Shibrot T Metcalfe G Wolf J E and Ottino 1996, “Mixing of granular Materials in Slowly Rotated Containers,” V42 No 12, pp 3351-3363.

Mc Ivor, R E, June, 1983, “Effect of Speed and Liner Configuration on Ball Mill Performance” Mining Engineering, pp617-622.

Mishra, B.K., and Rajamani, R.K., 1993, “Simulation of Balls in Ball Mills Part 1: Experimental Verification”, International Journal of Mineral Processing, V40, pp171-186.

Nityanand, N, Maney, B and Henein, H, 1986, “Analysis of radial segregation of different sized spherical solids in rotary cylinders,” Metallurgical Transactions B, 17B pp247-251.

Ottino, J M and Kharkhr, D V, 2000, “Mixing and Segregation of Granular Materials,” Annual Review of Fluid Mechanics, V32 pp55-91.

Poux M, Fayolle, P Betrand, J and Bridoux D and Bousquet, J, 1991, “Powder Mixing: Some Practical Rules Applied to Agitated systems,” Powder Technology, V 68 pp213-241.

Powell, M.S. and Nurick, G.N., 1996, “A Study of Charge Motion in Rotary Mills Part 1 – Extension of the Theory”, Minerals Engineering, V9, No. 2, pp259-268.

Powell, M.S. and Nurick, G.N., 1996, “A Study of Charge Motion in Rotary Mills Part 2 – Experimental Work”, Minerals Engineering, V9, No. 3, pp343-350..

Powell, M.S. and Nurick, G.N., 1996, “A Study of Charge Motion in Rotary Mills Part 3 –Analysis of Results”, Minerals Engineering, V9, No. 4, pp399-418

Roger, A. R, and Clements, J, A, 1971/72, “Examination of Segregation of Granular Materials in a Tumbling Mixer,” Powder Technology, V5, pp167-178.

Roger, R S C and Gardner R P, 1979, “A Monte Carlo Method for Simulating Dispersion and Transport through Horizontal Rotating Cylinders,” Powder Technology, V23 pp159-167.

Rogovin, Z., and Hogg, R., 1988, “Internal Classification in Tumbling Grinding Mills”, Powder Technology, V56, pp179-189

Sherritt, R G, Chaouki, J Mehrotrak, Behiela, 2003, “Axial Dispersion in the Three Dimensional Mixing of Particles in a Rotating Drum Reactor”, Chemical Engineering Science, V58, pp401-415.

Shoji, K, Hogg, R and Austin L G 1973, “Axial Mixing of Particles in Batch Ball Mills”, Powder Technology, V7 pp331-336.

Shoji et al, 1982, “Further studies of Ball and Powder Filling Effects in Ball Milling”, Powder Technology, V31, pp121-126.

Santomaso, A., Olivi, M., and Canu, P., 2005, “Mixing Kinetics Granular Materials in a Drum Operated in Rolling and Cataracting Regime ”, Powder Technology, V152, pp41-51.

Wightman, C., Muzzio, J.F., and Wilder, J., 1996, “A Quantitative Image Analysis Method for Characterising Mixture of Granular Materials”, Powder Technology, V89, pp165-176.

Weedon, D., M., 2001, “A perfect Mixing Matrix Model for Ball Mills”, Minerals Engineering, V14, No.10, pp1225-1236.

William, J.C., 1976, “The Segregation of Particulate Materials: A Review”, Powder Technology, V15, pp245-251.

NOMENCLATURE

$\Phi(t-\theta)$ = Tracer fraction per unit time from $\theta - \theta + t$

σ_o = Standard deviation for completely segregated sample

σ_R = Standard deviation for a randomly mixed sample

b_{ij} = Breakage function of particles of size *j* into *i*

$c_o(t)$ = Initial tracer concentration (gram tracer per gram solid)

$\Phi(t)$ = Mass fraction that has left the mill

τ = Mean residence time

ω = Rotational speed (rev/min)

σ = Standard deviation

$c_R(\theta)$ = Tracer proportion in the recycle stream

<*t*> = Mean residence time of the reactor

C = Circulation ratio

c(t) = Measured tracer concentration after time *t* of admission

*c** = Normalised dimensionless tracer concentration

D = Particle diffusion coefficient (m^2/s)

F = Powder feed rate (kg/s)

Fr = Froude number

g = Acceleration due to gravity

m = Number of reactors

I = mixing index

n = Smallest particle size range

S_i = Specific rate of breakage of particles in size class i

t = time (s)

v = Linear particle velocity (m/s)

W = Mill hold up (kg)

Z = Mill length

z = Particles axial location in the mill

N_c = Mill's critical speed, usually expressed as a percentage.

$k = \frac{qM_T}{m_1 m_2}$ (s^{-1}) is a quantity that defines the rate of mixing

q = mass flow into and out of the regions (kg/s)

m_1 & m_2 = Mass of particles in regions 1 and 2 respectively (kg)

M_T = Total mass of particles in the charge (kg)

m_t =Total mass of tracers in the charge (kg)

c_o = Steady state tracer concentration (kg/s)

c_1 = Tracer concentration due to region 1 (kg/s)

c_2 = Tracer concentration due to region 2 (kg/s)

c^* =Dimensionless tracer concentration, $c^* = \frac{c}{c_o}$

t_p =time at which tracer concentration reaches the peak point

ϕ_m = Differential RTD

APPENDIX 1: PROGRAMS USED FOR DATA ANALYSIS

THE FOLLOWING MATLAB PROGRAMME WAS USED TO ANALYSE TRACER CONCENTRATION FROM THE FRAMES OF A SPLIT VIDEO
The programme was divided into 5 sections, i.e.

- Read the frame from the specified path
- Convert the frames from RGB to Gray scale
- Scale the image
- Define the region of interest-ROI
- Read the mean Gray values of the pixels contained in the defined ROI
- Convert the Gray value intensities into concentration values

```
rgb1=imread('C:\My Documents\N50.jpg\0001.Jpg');  % the command reads the
frame
rgb2=imread( 'C:\My Documents\N50.jpg\0002.Jpg');
rgb3=imread( 'C:\My Documents\N50.jpg\0003.Jpg');
rgb4=imread( 'C:\My Documents\N50.jpg\0004.Jpg');
rgb5=imread( 'C:\My Documents\N50.jpg\0005.Jpg');
rgb6=imread( 'C:\My Documents\N50.jpg\0006.Jpg');
rgb7=imread( 'C:\My Documents\N50.jpg\0007.Jpg');
rgb8=imread( 'C:\My Documents\N50.jpg\0008.Jpg');
rgb9=imread( 'C:\My Documents\N50.jpg\0009.Jpg');
rgb10=imread( 'C:\My Documents\N50.jpg\0010.Jpg');

i1= rgb2gray(rgb1);
i2=rgb2gray(rgb2);
i3=rgb2gray(rgb3);
i4=rgb2gray(rgb4);
i5=rgb2gray(rgb5);
i6=rgb2gray(rgb6);
i7=rgb2gray(rgb7);
i8=rgb2gray(rgb8);
i9=rgb2gray(rgb9);
i10=rgb2gray(rgb10);

x=[0.5 720.5];
y=[0.5 576.5];

image(i1, 'Xdata', x, 'Ydata', y); axis image;
image(i2, 'Xdata', x, 'Ydata', y); axis image;
image(i3, 'Xdata', x, 'Ydata', y); axis image;
image(i4, 'Xdata', x, 'Ydata', y); axis image;
image(i5, 'Xdata', x, 'Ydata', y); axis image;
```

```
image(i6, 'Xdata', x, 'Ydata', y); axis image;
image(i7, 'Xdata', x, 'Ydata', y); axis image;
image(i8, 'Xdata', x, 'Ydata', y); axis image;
image(i9, 'Xdata', x, 'Ydata', y); axis image;
image(i10, 'Xdata', x, 'Ydata', y); axis image;

n=491;
m=326;
I1=imcrop (i1, [n,m, 16, 16]);
I2=imcrop (i2, [n,m, 16, 16]);
I3=imcrop (i3, [n,m, 16, 16]);
I4=imcrop (i4, [n,m, 16, 16]);
I5=imcrop (i5, [n,m, 16, 16]);
I6=imcrop (i6, [n,m, 16, 16]);
I7=imcrop (i7, [n,m, 16, 16]);
I8=imcrop (i8, [n,m, 16, 16]);
I9=imcrop (i9, [n,m, 16, 16]);
I10=imcrop (i10, [n,m, 16, 16]);

p1=mean(I1);
p2=mean(I2);
p3=mean(I3);
p4=mean(I4);
p5=mean(I5);
p6=mean(I6);
p7=mean(I7);
p8=mean(I8);
p9=mean(I9);
p10=mean(I10);

a1=mean(p1);
a2=mean(p2);
a3=mean(p3);
a4=mean(p4);
a5=mean(p5);
a6=mean(p6);
a7=mean(p7);
a8=mean(p8);
a9=mean(p9);
a10=mean(p10);

c = [a1;a2;a3;a4;a5;a6;a7;a8;a9;a10];
p=[0.004 0.4225 -53.445];
pts = polyval(p,c);
n=pts/10,
```

THE FOLLOWING MATLAB PROGRAMME WAS USED TO ANALYSE TRACER CONCENTRATION FROM THE DEM SIMULATIONS.

The programme was divided into 5 sections, i.e.

- Read the frame from the specified path
- Define the grinding media and particles
- Define the region of interest-ROI
- Determine the number of particles in ROI
- Calculate the dimensionless tracer concentration

```
x=dlmread('c:\clement\ccc.txt',',',4,0); % reads the file in the specified route.
j=0;
z=0;
for s=39:99
   for t=40:100
b=x(((30942*s)+1):3:(30942*t),:);            %creates a file b containing balls only.
ball positions are after 3 lines thats so hence reading at a range of 3

for n=1:10314;
   b(n,4)=n;              % a 4th row containing numbers as specified by n.
   y=b;                   %reads file b and stores it as m.
end

w=dlmread('c:\clement\myinput.txt'); %w(:,4);       % gets the numbers of the tracers
input=w(:,1);
%end
k=0;                      % initialises the value of k.
a=[0 0 0 0];                  %initialises the vector values of a..
for c=1:10314;
   if y(c,1)>0.18;       % sets the minimum value of roi in the x direction.
     if y(c,1)<0.21;     %sets the maximum value of roi in the x direction.
      if y(c,2)>0.0154;    %sets the minimum value of roi in the y direction.
         if y(c,2)<0.0454;   %sets the maximum value of roi in the y direction.
            k=k+1;        %sets a counter  for k
            a(k,:)=y(c,:);  % reads the number of balls in roi.
            [e,f]=size(a);   %gets the number and columns contained in roi.
              e;       % the value e represents the total number of balls in roi.
         end
      end
   end                   % terminates the looping of for and if.
end
end
```

THE FOLLOWING MATLAB PROGRAMME WAS USED TO ANALYSE TRACER CONCENTRATION FROM THE DEM SIMULATIONS.

```
 data= a(:,4);                % creates a file containing only balls in the roi.
 results =intersect(input,data); % gets the intersection of two files and creates a file containing the common balls.
 [g,h] = size(results);          %it shows the number of rows and columns of the tracers in the roi.
 g;                       % is the number of tracers in the roi.
M= g/e;                % defines the mixing index.
j=j+1;
z(j,:)=M;
end
end
E=z(61:61:3721);
```

THE FOLLOWING MATLAB PROGRAMME WAS USED TO CREATE NEW TRACERS FROM THE DEM SIMULATIONS.

```
file=dlmread('my_tracers1.out');
DEM1=dlmread('c:\my documents\chilowa1.txt',',',4,0);   % reads file containing
frame 1
DEM2=dlmread('c:\my documents\chilowa2.txt',','); % reads the file containig frame
100.
frame1= DEM1(1:3:30942,:);                              % specifies frame 1.
frame100=DEM2(((60*30942)+1):3:(61*30942),:);        % specifies frame 100 in the
file

for c=1:10314;
   frame1(c,4)=c;              % adds a 4th row containing numbers as specified by c
   frame100(c,4)=c;
   FR1=frame1;                  %reads file b and stores it as frame 1.
   FR100=frame100;
end

p=0;
Data=[0 0 0 0];                % intialises the file n.
for g=1:1000;
   for c=1:10314;
   if file(g,4)==FR100(c,4);          % compares balls in frame 1 and frame 100.
      p=p+1;
      Data(p,:)=FR100(c,:);       % creates the file for tracer particles and position
found frame 100.
   end
end
end

r=0;
TR=[0 0 0 0];                  % initialises the next tracer particles
for g=1:1000;
   for c=1:10314;
   if abs(Data(g,1)-FR1(c,1))<0.0045;    % creates a file of particles whose difference
is less than the abs value of 0.0003
      if abs(Data(g,2)-FR1(c,2))<0.0045;
     if abs(Data(g,3)-FR1(c,3))<0.0045;
         r=r+1;
      TR(r,:)=FR1(c,:);           % creates a file of new tracers.

           end
```

```
end
end
end
end

charge=sortrows(TR,[1 2]);
 n=length(charge);
 charge(n+4,:)=0;

 for v=1:n;
    if charge(v,:)==[0 0 0 0];
       break
    elseif charge(v,:)==charge(v+1,:);
       charge(v+1,:)=[];
       k=length(charge);
    end
end



for z=1:k;
    if charge(z,:)==[0 0 0 0];
       break
    elseif charge(z,:)==charge(z+1,:);
       charge(z+1,:)=[];
       q=length(charge);
    end
end

t=0;
particles=[0 0 0 0];
for s=1:q;
if charge(s,4)>388;
    t=t+1;
    particles(t,:)=charge(s,:);
end
end

u=0;
tracers=[0 0 0 0];
for g=1:1000;
    u=u+1;
    tracers(u,:)=particles(g,:);
end
save my_tracers2.out tracers -ASCII;
```

APPENDIX 2; LIST OF FIGURES

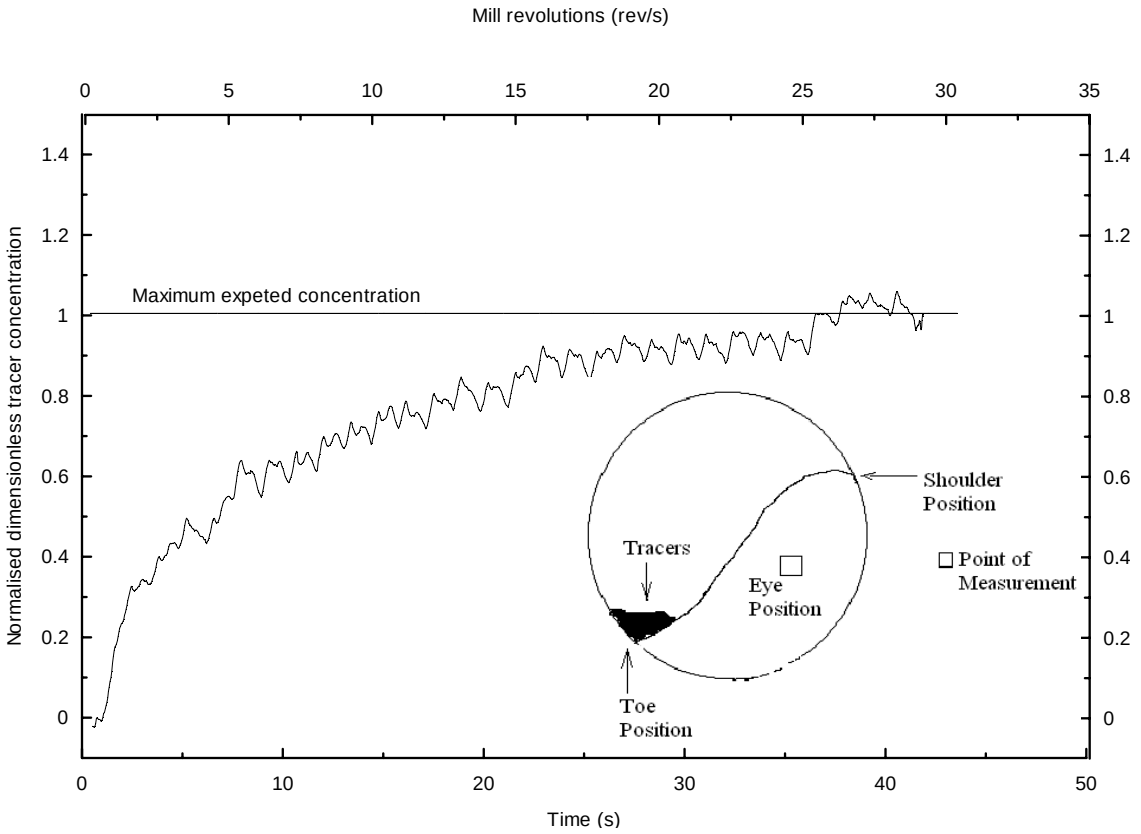

Figure A3.1; A plot of moving average data points for the mixing of tracer particles measured at the eye position showing the steady increase of tracer concentration for a mill operated at N_c=75%, ball load, J=0.2, and particle filling of U=1.0.

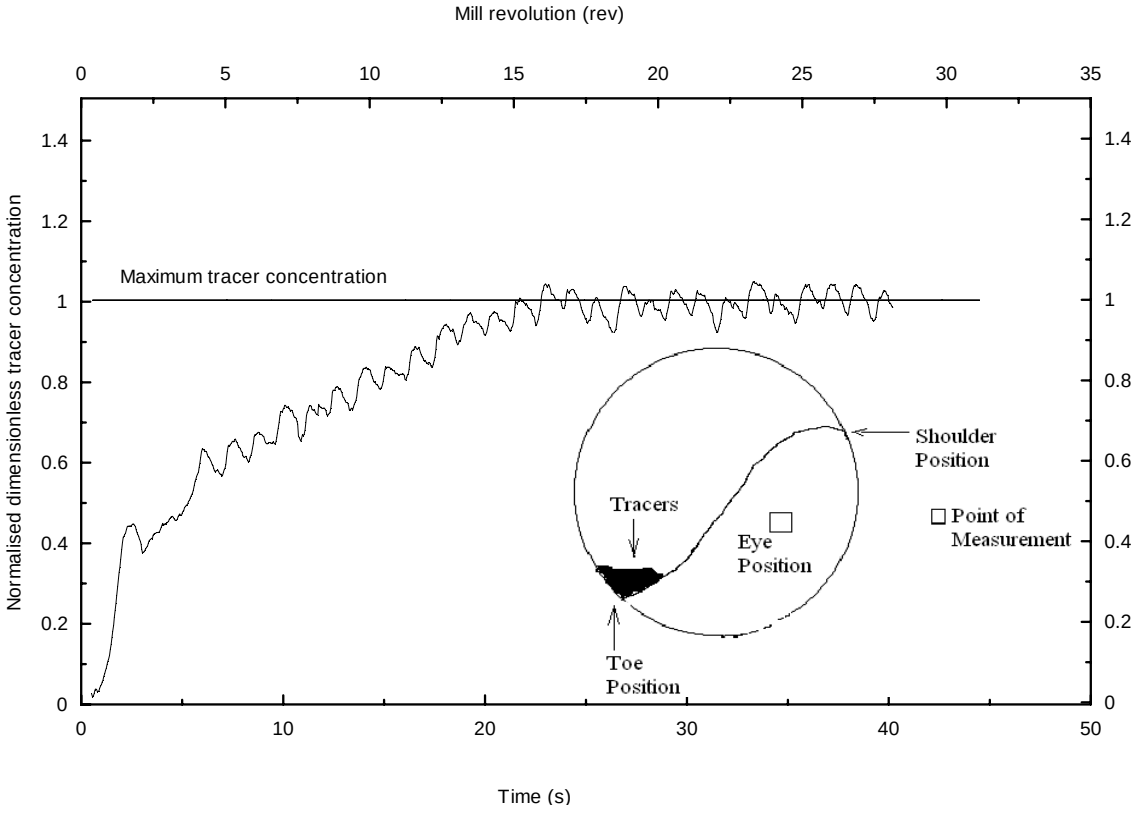

Figure A3.2; A plot of moving average data points for the mixing of tracer particles measured at the eye position showing the steady increase of tracer concentration for a mill operated at N_c=80%, ball load, J=0.2, and particle filling of U=1.0.

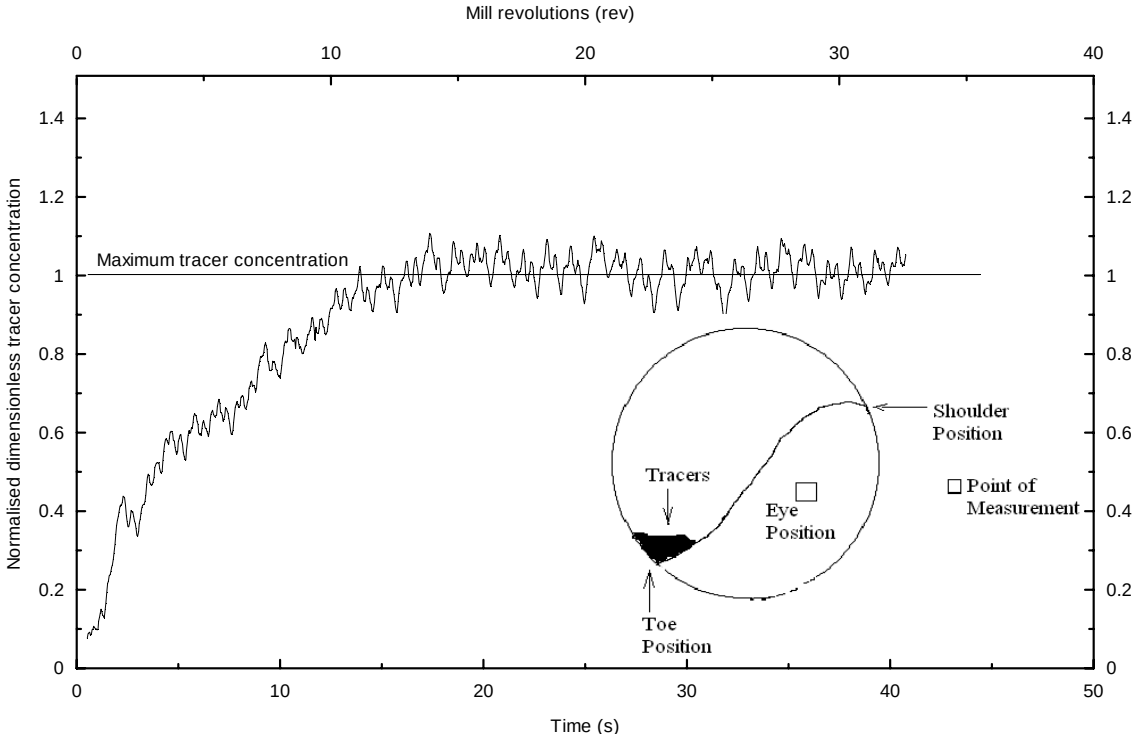

Figure A3.3; A plot of moving average data points for the mixing of tracer particles measured at the eye position showing the steady increase of tracer concentration for a mill operated at N_c=90%, ball load, J=0.2, and particle filling of U=1.0.

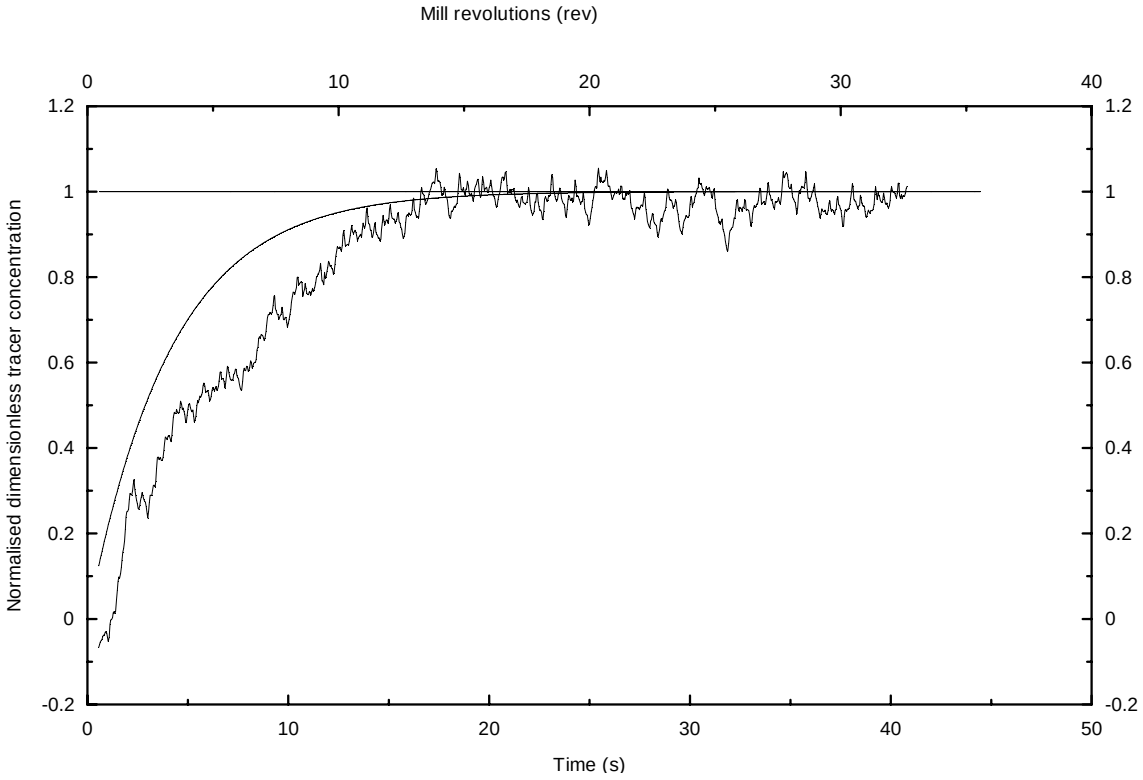

Figure A3.4; Radial mixing model was fitted with experimental data measured at the eye position of the charge giving k=0.19174 (s^{-1}) at N_c=90%, J=0.2 and U=1.

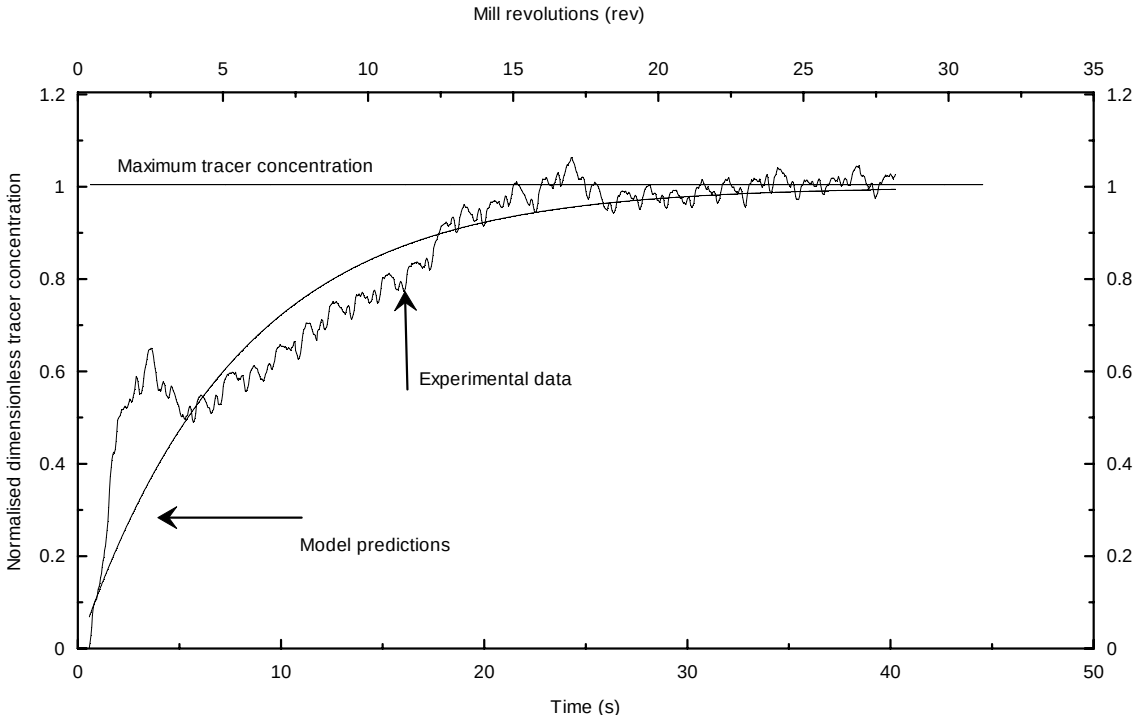

Figure A3.5; Radial mixing model was fitted with experimental data measured at the eye position of the charge giving k=0.130846 (s^{-1}) at N_c=80%, J=0.2 and U=1.

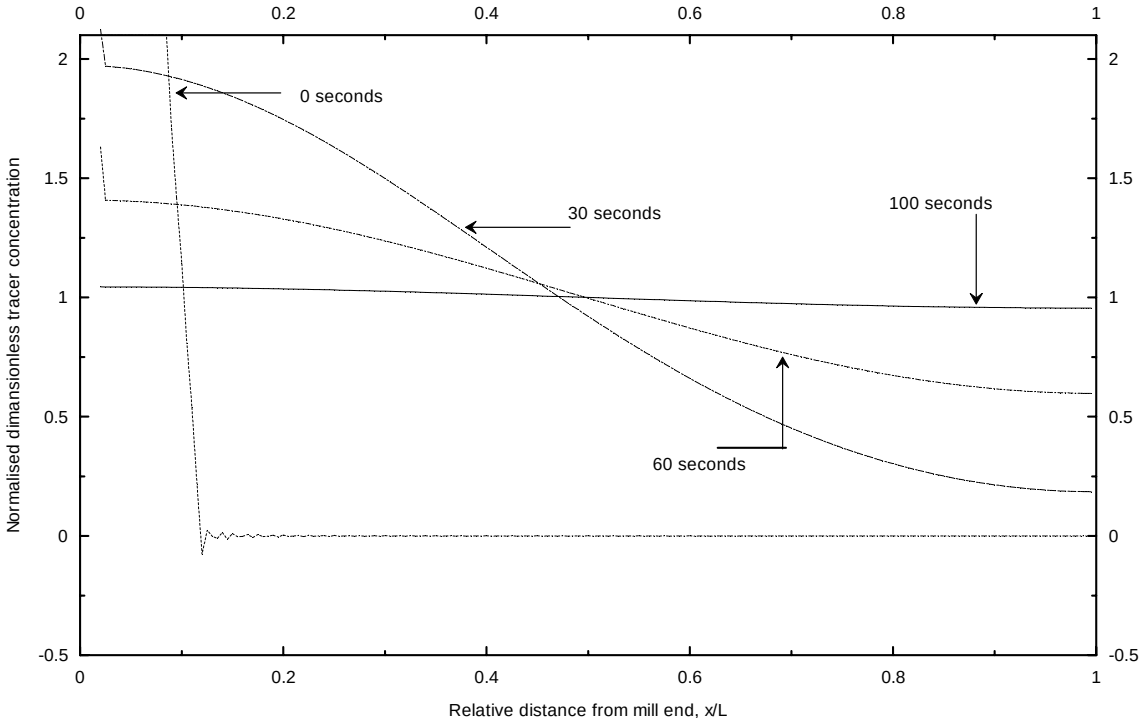

Figure A3.6; A plot of data obtained from the prediction of the axial dispersion model using method 2 measured at different times of mixing in mill operated at N_c=75%, ball load, J=0.2, and particle filling of U=1.0.

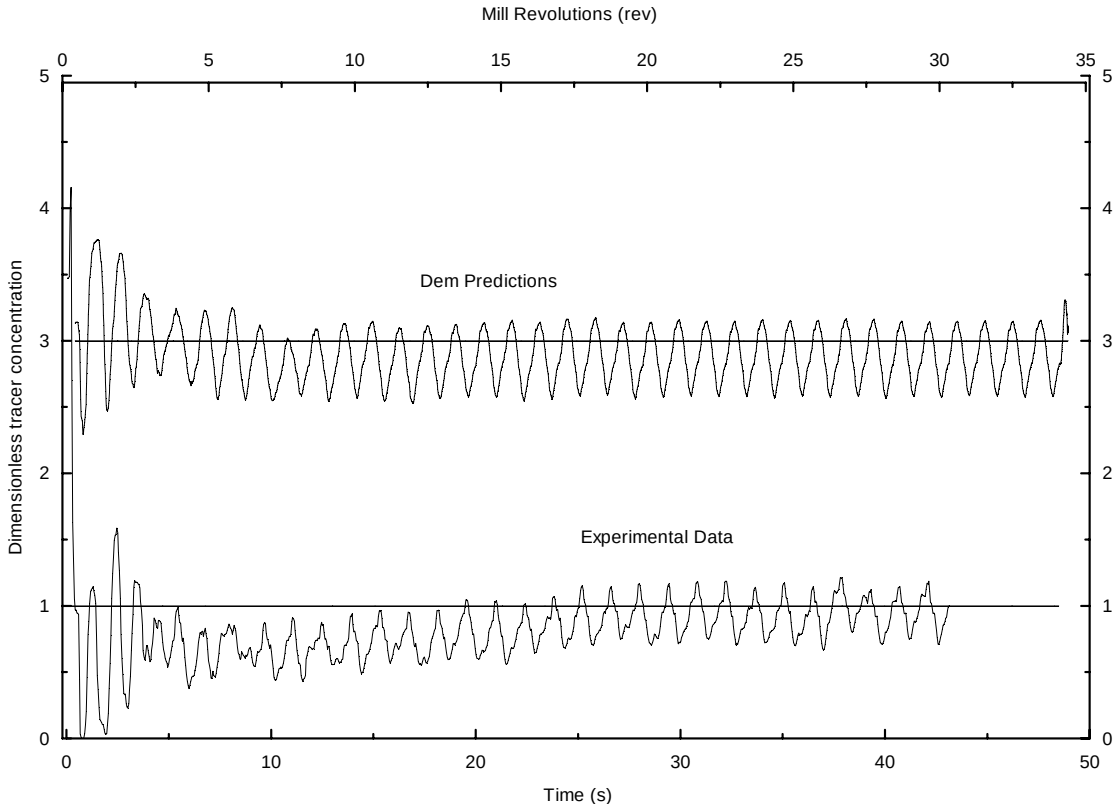

Figure A3.7; A comparison plot for experimental and DEM predictions for the mixing of tracer particles in mill operated at N_c=75%, ball load, J=0.2, and particle filling of U=1.0 (moving average data points). The graph has been moved 2 points up for clarity.

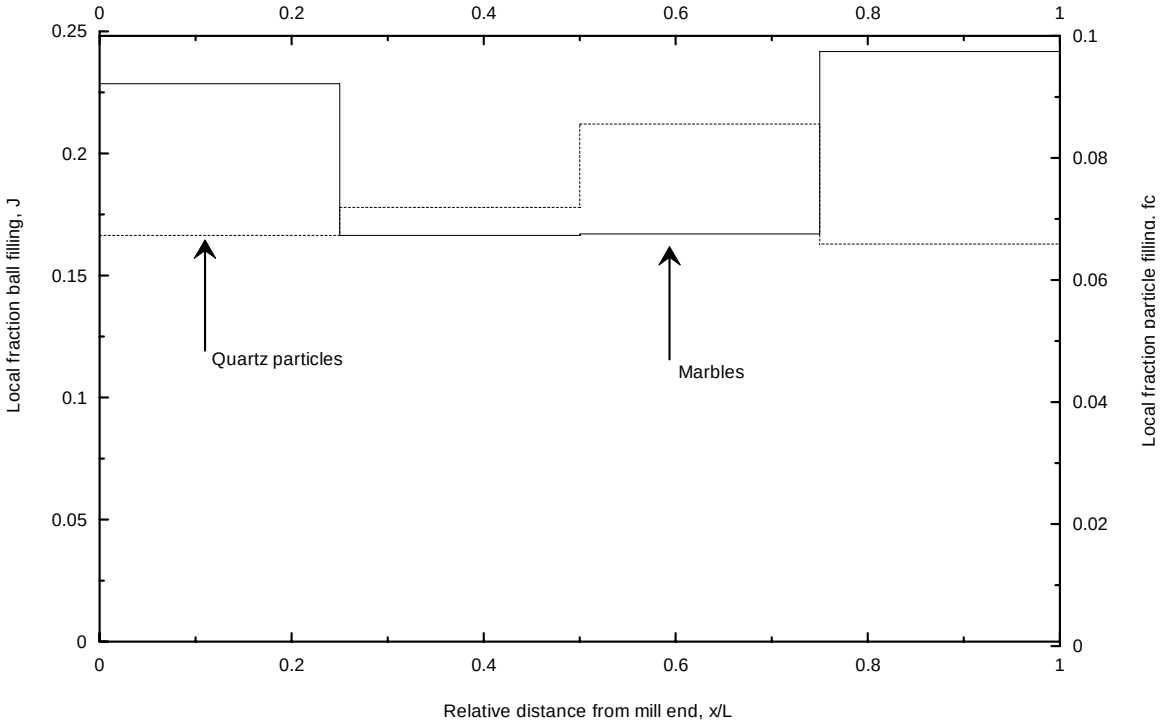

Figure A3.8; Axial distribution of particles and marbles after 5minutes of mixing for J=0.2, f_c=0.08 and N_c= 75% showing their tendency to segregate along the mill (steel balls – quartz charge system).